RISK ASSESSMENT AND EVALUATION OF THE CONDUCTOR SETTING DEPTH IN SHALLOW WATER, GULF OF MEXICO

A Thesis

by

YONG B. TU

Submitted to the Office of Graduate Studies of
Texas A&M University
in partial fulfillment of the requirements for the degree of

MASTER OF SCIENCE

May 2005

Major Subject: Petroleum Engineering

RISK ASSESSMENT AND EVALUATION OF THE CONDUCTOR SETTING DEPTH IN SHALLOW WATER, GULF OF MEXICO

A Thesis

by

YONG B. TU

Submitted to Texas A&M University
in partial fulfillment of the requirements
for the degree of

MASTER OF SCIENCE

Approved as to style and content by:

Jerome J. Schubert (Chair of Committee)	Hans C. Juvkam-Wold (Member)
Brian J. Willis (Member)	Stephen A. Holditch (Head of Department)

May 2005

Major Subject: Petroleum Engineering

ABSTRACT

Risk Assessment and Evaluation of the Conductor Setting Depth in Shallow Water, Gulf of Mexico.

(May 2005)

Yong B. Tu, B.S., Texas A&M University

Chair of Advisory Committee: Dr. Jerome J. Schubert

Factors related to operations of a well that impact drilling uncertainties in the shallow water region of the Gulf of Mexico (GOM) can be directly linked to the site specific issues; such as water depth and local geological depositional environments. Earlier risk assessment tools and general engineering practice guidelines for the determination of the conductor casing design were based more on traditional practices rather than sound engineering practices.

This study focuses on the rudimentary geological and engineering concepts to develop a methodology for the conductor setting depth criteria in the shallow water region of the GOM.

DEDICATION

I dedicate this work to my loving parents, my caring brother, and my understanding wife.

ACKNOWLEDGEMENTS

I wish to express my gratitude to the Mineral Management Services (MMS); who made this project possible.

My sincere admiration and thanks to Dr. Jerome J. Schubert for being my mentor, committee chair, principal investigator and friend.

To all my friends, I am grateful for all your kindness and encouragement!

Lastly, I would like to thank my family for their unconditional love and patience.

TABLE OF CONTENTS

Page

LIST OF FIGURES

LIST OF TABLES

Page

1 INTRODUCTION

Faced with geopolitical and global economic uncertainties, many leading exploration and production corporations (E&P) have placed deliberate emphasis on marketing their “shallow hazardous” and “economically volatile” assets to small independent E&P companies. However, due to recent technological advancements in production systems, it is economically feasible for small independent E&P companies to pursue these “unwanted” assets as part of own portfolio.

It is anticipated that these operators will introduce new wells into mature fields to perform further reservoir and geological testing and new development plans to the acquired assets. Early drilling studies and guidelines have mentioned casing design and well control issues. However, they have ignored situations where upward fluid migration can lead to abnormally pressured shallow formations, especially in a developed field. Even in situations where there has not been any artificial charging of shallow formations, selection of conductor and surface casing setting depths has, in the past, been based more on "rule of thumb" than sound engineering practices.

Risks associated with exploration and production of a hydrocarbon reservoir has been long accepted by the industry. Typically, one of the three risk assessment methods would be utilized to analyze an engineering problem and to provide a plausible solution.

- Sensitivity Analysis
- Risk-adjustment / Parametric method (i.e. expected value analysis)
- Stochastic Simulation (i.e. Monte Carlo Method)

Currently, HAZOP the technique of Hazard and Operability Studies are carried out for most drilling related risk assessments and analysis. This technique can be considered as a type of Risk-adjustment Analysis method. This technique can identify potential

---

This thesis follows the style and format of *SPE Drilling and Completion.*

hazards and operability problems caused by deviation from the design intent of both new and existing procedures.

This study will base on rudimentary engineering and geological theories and to provide a feasible engineering procedure for the conductor setting depth based on direct measurements, such as soil boring.

1.1 Background

Abnormally pressured formations can be found around the world, with varying degrees, in nearly all sedimentary basins. The distribution of known abnormally pressured formations is vast, not only dependent upon the geological scale, but also dependent on the vertical sedimentary interval from superficial levels down to greater depth.

In most of the cases, a closed or semi-closed environment is an essential prerequisite to the development and maintenance of abnormally pressured formations. It is the inability of fluids to escape from interstitial pore spaces of rock matrix and underlying compaction from the rock above that creates the abnormally pressured formation phenomenon.

Within the hydrocarbon reservoir systems, the consequences of abnormally pressured formations can be considered desirable and undesirable. The abnormal pressure would affect the hydrodynamics of the pressure gradient and its fluid migration within an enclosed reservoir. By utilizing this pressure, we could determine the efficiency of the boundary conditions for the hydrocarbon system. However, its unpredictable and unquantifiable nature would be hazardous to the daily drilling operations.

In the past, drilling in an abnormally pressured basin utilized a couple of "recommended" methods; "drilling for the kick" and "overbalanced drilling". Just as the names suggested, "drilling for the kick" consist of using minimum mud-weight/hydrostatic pressure to overcome the formation pressure to achieve a faster Rate of Penetration (ROP). Hence the possibility of encountering a kick from the formation is ignored. The well can be shut-in and formation pressure can be calculated for the need to increase mud weight. This method could lead to an unintentional and uncontrollable blow-out. The "overbalanced drilling" method contrary to the "drilling for the kick" method is to keep the mud weight/hydrostatic pressure within the wellbore very high in order to reduce the chances of kick and blowouts. This method could lead to unintentional fracturing of the wellbore in the shallow water of the GOM and provide fractured tunnels for fluids migration in both vertical and horizontal directions. These two drilling methods should not be considered for shallow water GOM drilling operations due to lack of concerns toward the shallow marine depositional environments, and health, safety and environment surrounding the drilling location.

1.2 Blowout Statistics

An influx of formation fluids into the wellbore is, in most cases, a precursor to each of the blowouts recorded and analyzed in the Danenberger study[1]. The blowout data collected were from the period of 1971 to 1991. A total of 87 blowouts (Table 1-1) occurred during drilling operations on the Outer Continental Shelf (OCS) of the United States. Eleven of the blowouts resulted in casualties. Danenberger identified the majority of the blowouts were attributed to shallow gas influxes and were of short duration. The study also grouped shallow gas blowouts by geological age of the well production. (Table 1-2)

Table 1-1 Boreholes with Spud Dates of 1971 to 1991, Danenberger[1]

Water Depth (ft)	Wells			Total Wells	Total Blowouts	Wells Per Blowouts
	Exp	Dev	Sulfur			
0-200	4744	8120	148	13012	39	334
201-500	2312	4599	49	6960	38	183
501-1000	395	251	-	746	8	93
> 1000	496	222	-	718	2	359
Total	7947	13292	197	21436	**87**	246 (mean)

Table 1-2 Shallow Gas Blowouts by Geological Time of Well Production, 1971-1991, Danenberger[1]

Epoch	Wells Drilled	Shallow Gas Blowouts	Wells per Blowouts
Pleistocene	9892	37	267
Pliocene	3831	12	319
Miocene	6723	8	840

Hughes[2] analyzed approximately 400 Gulf Coast blowout events within the time frame between July 1960 and Jan 1985. A total of 121 blowouts were in the OCS, 77% of the cases were gaseous fluids produced during the actual blowouts. Only 20% of the reported blowouts' activity just prior to the event was related to drilling. However, the majority of these blowouts bridged naturally.

In 1995, the Mineral Management Services (MMS) initiated the MMS Technical Information Management System (TIMS). The TIMS provides the general public with investigation reports for losses of well control in both the GOM region and Pacific region (PAC) while providing an accounting method for blowout events within these regions. The aim of the TIMS is to provide safety alerts and investigation reports for all losses of well control events within its jurisdiction.

Table 1-3 TIMS Losses of Well Control[3]

Losses of Well Control													
	1992	**1993**	**1994**	**1995**	**1996**	**1997**	**1998**	**1999**	**2000**	**2001**	**2002**	**2003**	**2004**
GOM	3	3	0	1	4	5	6	5	8	9	6	4	2
PAC	0	0	0	0	0	0	1	0	1	1	0	0	0
Total	3	3	0	1	4	5	7	5	9	10	6	4	2

From Table 1-3, there were total occurrences of 59 "losses of well control" events between 1992 and 2004 for both GOM and PAC regions;

- The majority of the events took place in less than 500 ft of water depth
- 56 (95%) events occurred in GOM region
- 34 out of 56 GOM events were related to drilling activities, and
- 8 out of 34 events occurred prior to, during and/or just after cementing operations.
- Approximately 2 out of 56 GOM events resulted in fire and temporarily abandonment from the rig/location
- 1 event reported financial losses of 2 million USD

1.3 Causes of Shallow Gas Kicks

One of the most critical problems for exploration and development of hydrocarbons in shallow-water of the GOM is detection of geopressures prior to the actual drilling operations[4,5,6,7]. The physical basis for the determination of porosity and pore pressures from seismic measurements has been the often observed correlation between seismic velocity and porosity and between porosity and effective pressure[8,9,10]. In most cases, the high pressured zones are often associated with high porosities and low seismic velocity. Hence, improper interpretation between seismic velocity and porosity could underestimate existing geopressures along the planned wellbore. Trapping mechanisms such as lenticular sand pockets, sealing faults with massive surrounding shale, and dense caprock are just a few of the possibilities for the generation of abnormally pressured

formations. It is illustrated in Figure 1-1 the lenticular sand pocket penetrated by a wellbore along a planned well path.

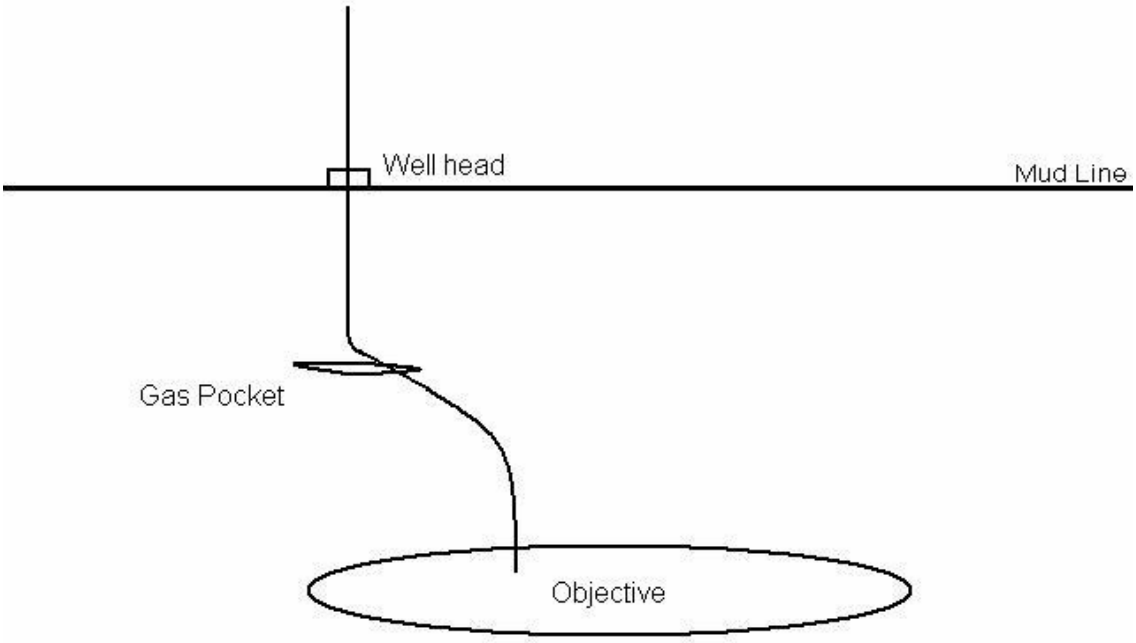

Figure 1-1 Shallow "Lenticular" Gas Pocket

According to a study of 172 blowouts worldwide by the Norwegian Sintef Research Organization, shallow geo-hazard is the most serious single cause of kicks leading to blowouts[7]. Goins[7] (1987) illustrated the low margin of overbalance in shallow depth and structural overpressures coupled with poor drilling practices were the causes of formation kicks that could lead to losses of control of well. The poor drilling practices included, but are not limited to, a lack of attention to drilled gas, swabbing and hole-filling that could lead to loss of circulation.

Exiting trapped geopressures, lack of attention to drilling operations coupled with smaller tolerance between pore pressure and fracture pressure causing narrow pressure margins while drilling could lead to a well control event for the operator.

1.4 Objectives of the Study

This study will define the geological settings along with the depositional environment required for the potential causes of abnormally pressured formations in the shallow water of the GOM.

To establish engineering concepts relevant to pore-pressure gradient, overburden pressure gradient, fracture gradient and Poisson's ratio. Hence, utilizing these concepts and methodologies, within the confines of this study is to establish engineering guidelines for the selection of conductor setting depth in the shallow waters of GOM.

1.5 Expected Contribution from the Study

The sponsor of this project, MMS, would have an important document and guideline for its role in evaluation of the risks involved with conductor casing setting depth criteria.

The petroleum E&P industry would have accesses to a well written document that could be utilized by drilling engineers and companies alike as a guideline for the development of well plans and well contingency plans.

2 GEOPRESSURE, STRESS AND FRACTURE CONCEPTS

Over the centuries, pressure and stress theories and their explanations have been proposed and many predictive methods have been advocated via technical journals. In this section, the basic formation pressure and stress concepts will be introduced and analyzed for both hydrostatic and non-hydrostatic pressure concepts. This would be an essential step towards a better understanding of engineering evaluation for the conductor setting depth criteria.

2.1 Definitions

2.1.1 Hydrostatic Pressure

Pressure is commonly understood as force per unit area. By the same token, the hydrostatic pressure (P_h) is the pressure exerted by the weight of the fluid on a static surface. This force is a function of vertical height of the column and fluid density. The geometrical sizes of the fluid column do not affect the hydrostatic pressure exerted on a known surface. The mathematical expression for this relation is

$$P_h = \rho g h, \quad \text{.....(1)}$$

where P_h = hydrostatics pressure

ρ = fluid density

h = vertical height of the fluid column

g = gravity

2.1.2 Pore Pressure

Pore pressure (P_p), sometimes called formation or formation-fluid pressure, is defined as the pressure contained in the pore space of subsurface rock[1]. There are roughly three categories of formation pressure:

- Subnormal formation pressure is the formation pressure less than hydrostatic pressure
- Normal pore pressure are functions of formation hydrostatic pressure and interstitial pore fluid density
- Abnormal formation pressure (geopressures) is pressure greater than the hydrostatic pressure of the formation fluid in the geological facies. This anomaly is limited by overburden pressure.

2.1.3 Overburden Pressure

Overburden pressure (S) at a given depth is the pressure exerted by the weight of the overlying sediments on the interstitial fluids. Since this is not a fluid dependent pressure it is often preferable to utilizing the rock matrix bulk density, ρ_b, term to express in a mathematical formula as the following

$$S = \rho_b D\,, \quad \text{.....(2)}$$

where, ρ_b = formation bulk density

D = vertical thickness of the overlying sediments

The bulk density of the sediment is a function of rock matrix density, pore-fluid density and porosity within the confines of the pore spaces. The mathematical expression of

$$\rho_b = \phi\rho_f + (1-\phi)\rho_m\,, \quad \text{.....(3)}$$

where, ϕ = rock porosity

ρ_f = formation fluid density

ρ_m = rock matrix density

can be used for rock bulk density calculation. A decrease in porosity is necessarily accompanied by an increase in bulk density.

From Eq. 2 and Eq. 3, the proportional relationship between burial depth and overburden pressure can be visualized. For clays, the reduction is weight dependent. If clay porosity and depth are represented on a arithmetical scales, the relationship between these two parameters is an exponential function. On the other hand, for porosity expressed logarithmically, the porosity-depth relationship is approximately linear. In the case of sandstone and carbonates, the relationship is a function of many parameters other than simply compaction from burial depth. Pore fluid composition, diagenesis effects, and sediment sorting are just few examples of the complex parameters associated with sandstone and carbonates.

In shallow water depositional environments, the upper part of the sedimentary column, the bulk density gradients increase much steeper than at greater depth. This phenomenon is due to the superficial seawater saturated interval close to the sea floor.

2.1.4 Pressure Gradients

The pressure gradient concept was to provide a degree of consistency to pressure data and simplification of pressure calculations. It is simply expressed as pressure over depth.

2.2 Geopressure – The Origins

Abnormal pressure has many origins. The abnormal pressure or geopressures are hydrodynamic phenomena which at time can play a major factor, along with a semi-closed environment for the existence and maintenance of this phenomenon. The ability of this semi-closed environment to resist the expulsion of formation fluids, implying that drainage is inadequate with respect to time. Since it is rarely for a rock to be totally impermeable, minerals such as clay allows fluid transfer on a geological time scale. However, it's effectiveness as a seal is dependent upon the thickness and capillarity of the formation rock.

In this section, several mechanisms leading to abnormal formation pressure will be examined in order to understand the origin of the phenomena in the shallow waters of GOM.

- The overburden effect
- Aquathermal Expansion
- Clay diagenesis
- Osmosis
- Evaporite Deposits
- Organic matter transformation
- Tectonics

2.2.1 The Overburden Effect

Under normal conditions, when sediments compact normally, their porosity is reduced at the same time as pore fluid are being expelled from the pore spaces of the formation. Previous studies [2,11,12] have confirmed the reduction of porosity with increase of burial depth of sediment. Some studies have indicated a result from 80% porosity for argillaceous ooze just below the seafloor to an average value of 20% to 30% a few thousand feet beneath the seafloor. Indication of gradual porosity reduction at greater

depth is also strong. Hence, reduction in formation porosity is an indication of an increase bulk density of the formation.

In general, permeability, formation drainage efficiency, sedimentation, and burial rate must achieve an overall balance before normal compaction can be realized. Therefore, the more recent the active phase subsidence, the greater chance of abnormal pressure being encountered; recent deltaic formations, passive continental margins and accretion of subduction zones are just a few examples of geological facies that have the potential for abnormally pressured formations.

One of the governing factors for abnormal pressure is the presence of drainage within the argillaceous facies. The fluid pressure within the argillaceous facies is often assumed to be very similar to the adjacent sand body with which it is in contact. It is then plausible to relate the magnitude of abnormal pressure appeared to be related to the ratio of sand to clay in a sedimentation series.

Overall, the magnitude for abnormally pressured formations can be contributed to the imbalance between the rates of subsidence and dewatering efficiency of the formation. This can be considered the most frequent cause of abnormally pressured formation around the world and in the younger shallow formations of the GOM.

2.2.2 Organic Matter Transformation

At shallow depth, organic matter contained in the sediments is broken down by bacterial action, generating biogenic methane. In a closed environment, the biogenic gas expansion could lead to an abnormally pressured formation. The thermo generation of light hydrocarbons such as methane proceeds at an increasing rate as temperature rises. The process would usually last utill the exhausting of the heavy hydrocarbons within the

system. As long as the system is sufficiently confined and enough organic matter is present in the system, the gas expansion can develop in the shale sand series of GOM.

2.2.3 Clay Diagenesis

Unlike the concept of overburden effect, the clay diagenesis conceptualizes on a microstructure level rather than a geological facies. Physical correlation between a high geothermal gradient and clay diagenesis can be realized by investigating an abnormally high porosity of under-compacted zones and its association with a steep abnormal gradient. This factor can enhance the dewatering and transformation of montmorillonite. However, abnormal pressure retards dewatering and increases salinity, tending to alter the diagenetic process by comparison with an unsealed environment. Hence, the clay transformation and dewatering in the course of diagenesis are often considered a contributory factor in the generation of abnormal pressure rather than a major cause of abnormally charged formation.

2.2.4 Osmosis

The concept of osmosis has been known since the 18th century. This concept can be loosely defined as a spontaneous transfer of one concentration of fluid to another fluid via a semi-permeable membrane. Past studies had shown the flow of water through a clay bed is dependent on four factors, differential pressure, differential concentration, differential electrical charge potential, and temperature within the formation. The flow potential could result in over-pressuring shale and has been attributed as a source for abnormal pressures in the San Juan basin[13].

It seems that the capability of osmosis to create an abnormally pressured formation in the GOM is limited to special cases such as sharply contrasting salinity, and proximity to salt domes structures in the GOM. This is particularly evident to the GOM depositional environment where the Louann Salt play has been a major hydrocarbon indicator in the

region. However, in most of cases, the role of osmosis is difficult to prove and must be considered as a minor effect to the overall abnormally pressured formations.

2.2.5 Evaporite Deposits

Two roles of evaporite deposits would affect the pressure gradient of the formation, one is a passive role as a seal, and another is an active role as a pressure generator. Total impermeability and high mobility are two key physical characteristics that defined evaporite deposits as a potential seal.

The pressure generation by means of diagenesis can be realized with chemical water production within the confines of the formation. For example, anhydrite rehydration is usually accompanied by an increase in volume of formation water. If the pore space is constant, then an increase of volume means a direct increase in pore pressure. This type of abnormal pressure generation is not likely in the shallow water of the GOM.

2.2.6 Aquathermal Expansion

This concept results from the consequence of the expansion of water due to the thermal effect in a constant and isolated pore volume within a formation. It is commonly believed that strong thermal anomalies, such as volcanic activities around the region, can create a local overpressure of a limited time frame.

For propose of this study, in the shallow water of GOM region, the impervious formations are extremely rare coupled with lack of thermal anomalies in the region that leads to the unlikeliest of aquathermal expansion in the formations of the shallow water, GOM.

2.2.7 Tectonics

In general, tectonic movement causes rock deformation which has a direct or indirect effect on the fluid pressure distribution; this means that tectonics may create abnormal pressure anomalies or restore pressure to normal by means of faulting and fracturing of formations. (Figure 2-1)

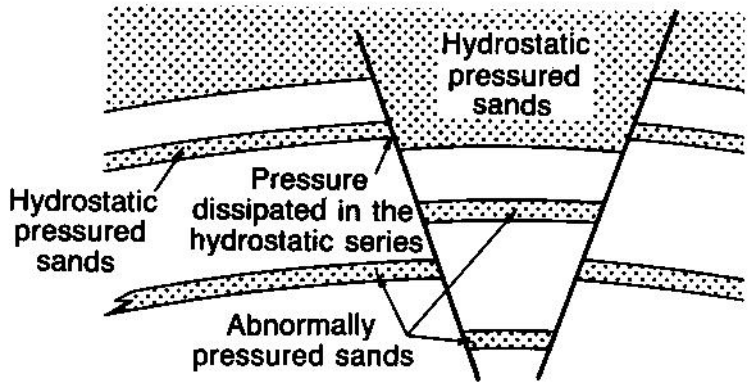

Figure 2-1 Relationship between faulting, fracturing and pressure

The relationship between tectonic movements and sedimentation is more evident in the development of a delta, such as the Mississippi River delta in the GOM. This is due to the need to achieve equilibrium between the sedimentation rate, subsidence rate and sea level. Such environments encourage the formation of under-compacted zones within the deltaic facies. They form either under-drained or un-drained parts of the delta. Dependent on the direction of sediment flow, a proximal zone and distal zone can be observed. The growth faults will develop preferentially in a proximal zone, whereas shale domes and ridges can be developed in the distal zone.

Growth faults posses a curved faulting plan which is invariably concave towards the basin. This plan is nearly vertical in its upper part, and then tends gradually to conform to the dip of strata. The preferential site for hydrocarbon accumulation is located at the down-dip compartment against the fault. If this type of structure is penetrated during a

drilling operation, there will always be the risk of crossing into the under-compacted shale, thus risk a sudden rise in formation pressure.

Shale domes are the result of intrusive upward migration of underlying layers. They are always under-compacted and hence always abnormally charged with pressure. Mud volcanoes are the ultimate manifestation of clay diapirism. They tend to be situated along large, active transcurrent faults, such as in Caspian Sea, coastal region of Azerbaijan. Below is a picture of erupting mud volcano, taken approximately three years ago, near the City of Baku, Azerbaijan. (Figure 2-2) Mud volcano eruptions are extremely rare in the GOM, especially in the shallow marine environment.

In summary, tectonics and fluid pressures interact to give a variety of effects. The above mentioned is really the “tip of iceberg”. This is only used to demonstrate the importance of tectonic activities in relation with formation and its internal pressures.

Figure 2-2 Mud Volcano Eruption, Baku, Azerbaijan, Courtesy of R. Oskarsen and B. Mcelduff (2004)

2.2.8 Geopressures Summaries

Above are various ways in which abnormal pressure can arise and an attempted to distinguish between major and minor causes for the shallow marine depositional environment in the GOM region. Identifying the cause is generally a delicate matter, and calls for sound knowledge of the geology of the region. The crucial importance of seals and drains in developing and maintaining abnormal pressure has been demonstrated. Time is the determining factor in fluid dispersal, which explains why abnormal pressure is more commonly found in association with young sediments. Young clay-sand sequences can be found in deltas, passive continental margins, and accretion prisms of subduction trenches. High pressure may result from a combination of various causes and these are more likely to be found in clay-sandstone sequences because of mechanical,

physical and chemical properties of clays. All of these characterizations can be identified along the shallow marine depositional environment of the GOM.

2.3 Stress

The depositional environments are the basis for formation stresses and along with the earth's gravitational forces, stress fields were developed around the globe. There are many possibilities which lead to the creation of an abnormal, a normal, or a subnormal formation pressure. These types of information are pertinent for engineering problem solving, such as drilling engineering and fracture analysis. The predictions and or estimation of these engineering values, such as overburden pressure, fracture gradient, and pore pressure values, are critical to any E&P operations.

2.3.1 Stress and Strain

A material is considered in a state of stress, when a force in vector quantity defined in terms of magnitude and are direction applied to it. Hence, force acted to a specific point on a given surface and stress within a body was defined by normal and shear stresses on all planes.[14] To study the deformation of the subsurface materials, we have to consider the deformation characteristics of particular materials.[15,16,17,18,19,20]

A material is considered to behave in an elastic manner when a load applied to the material is removed, and the material returns to it original physical state without any permanent damage to the material. For most materials, once the loading response significantly deviates from linearity, then a plastic deformation of the material occurs. The point that signifies the initial deviation is the called yield point. The linear elastic material can be defined based on the linear characterization of the loading curve in the load vs. displacement diagram. (Figure 2-3) This linear elastic behavior persists as long as the load to the material is less than the yield point. The slope between the load

intensity vs. normal strain is defined as elastic modulus, often we refer to as Young's Modulus of the material. (Figure 2-4) The equation for E is given by

$$\frac{F}{A} = E\frac{\delta}{L}, \quad \text{.....(4)}$$

where, $\frac{F}{A}$ = Force Intensity, σ

E = Young's Modulus

$\frac{\delta}{L}$ = Normal Strain, ε

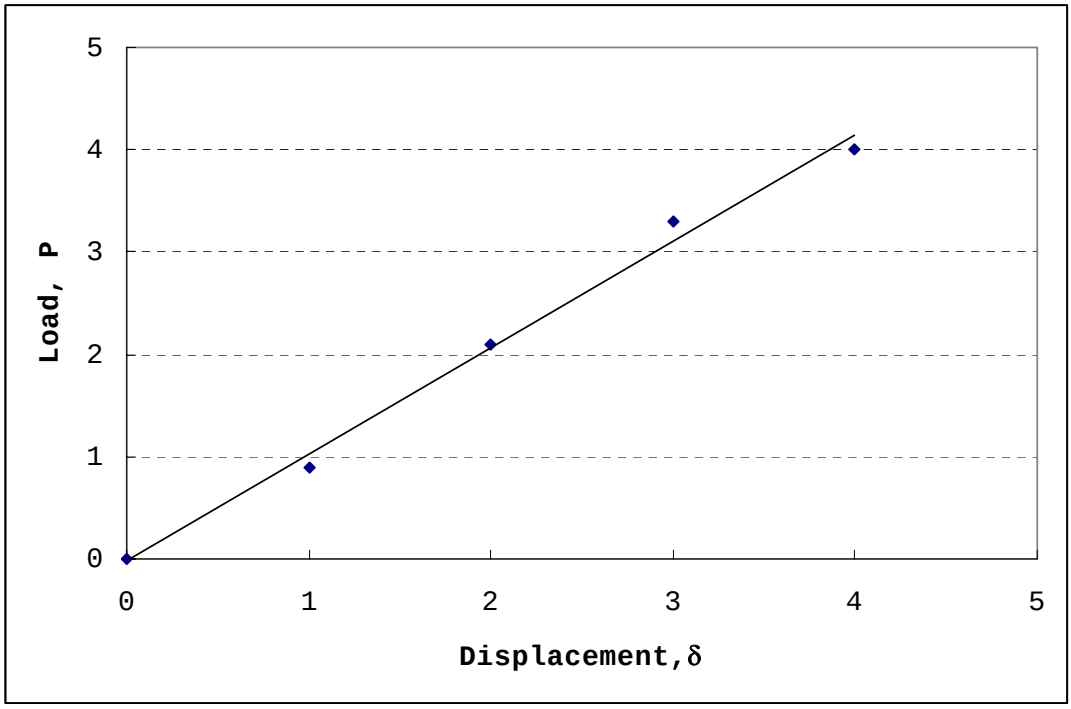

Figure 2-3 Load vs. Displacement diagram

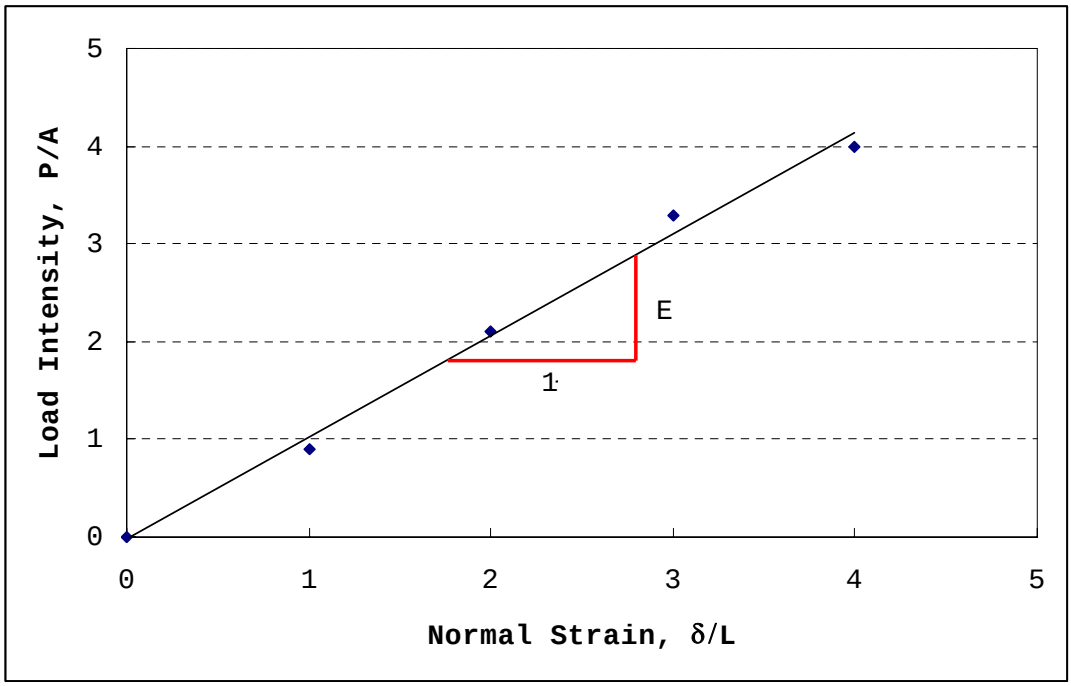

Figure 2-4 Load Intensity vs. Normal Strain

In the past, experiments have shown for a given isotropic material that the change in length per unit length of line elements in the perpendicular or transverse directions, are fixed fraction of the normal strain in the loaded direction. Hence for a given material, its elasticity is constant. This ratio was first defined by S.D. Poisson.[2,13,18,19,21]

$$\nu = -\frac{\varepsilon_{tr}}{\varepsilon_a}, \quad \text{.....(5)}$$

where, ε_{tr} = Transverses Strain

ε_a = Axial Strain

ν = Poisson's Ratio

This isotropic relation considered that the formation has not been a subject of any lateral deformation since sedimentation and it always deforms elastically during compaction.

In terms of drilling engineering, the elastic modulus is an important input parameter for a fracture width calculation during a hydraulic fracturing analysis; whereas Poisson's ratio is a property for prediction of the fracture gradient. Table 2-1; provides a good "rule of thumb" for engineers to determine the elastic modulus and Poisson's ratio during a calculation.

Table 2-1 Typical Elastic Properties of Rocks[13]

Rock Type	E (10^6 psi)	ν
Granite	3.7 to 10.0	0.125 to 0.25
Dolomite	2.8 to 11.9	0.08 to 0.2
Limestone	1.4 to 11.4	0.1 to 0.23
Sandstone	0.7 to 12.2	0.066 to 0.3
Shale	1.1 to 4.3	0.1 to 0.5

2.3.2 Rock Mechanics

In comparison with metallic alloys, the response of a rock element to stress depends on such things as its loading history, lithological constituents, cementing materials, porosity, and any inherent defects. Even so, similar stress/strain behavior is observed and much of the same terminology has been adopted in the field of rock mechanics

Rocks tend to be more ductile than plastic with increasing of confine stress and temperature.[13] An ideal plastic body does not yield until a particular load, the yield stress, has been applied. Most materials, including sedimentary rocks, that approach being plastic exhibit elastic characteristics below the yield point. Often formations are categorized as "brittle" or "plastic". The term brittle is typically used to describe hard rock and plastic or ductile is used loosely to describe soft rock.[20]

2.3.3 Horizontal and Vertical Rock Stress

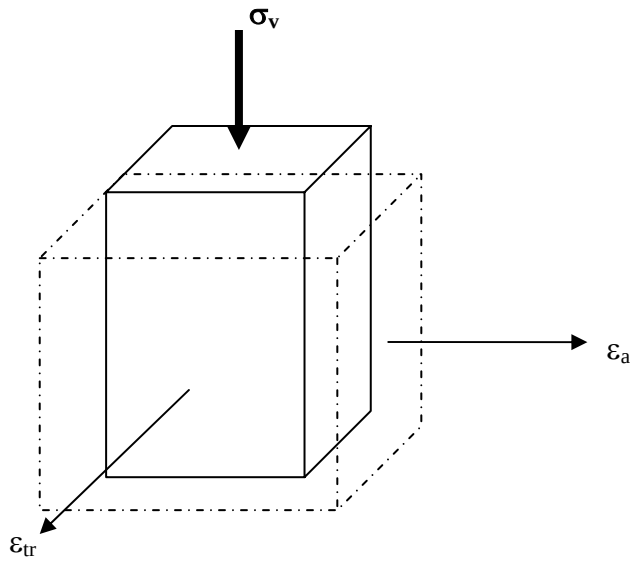

Figure 2-5 Transverse-Reaction Strain for a Confined Linear-Elastic Material

In general, the simplest rock fracturing model assumes the material is in a confined linear-elastic state, with respect to vertical overburden load. (Figure 2-5) In the scenario for the isotropic material, where axial strain has the same magnitude as the transverse strain, a horizontal strain can be used to generalize both axial and transverse strain.

$$\varepsilon_H = \varepsilon_a = \varepsilon_{tr}, \quad \text{.....(6)}$$

where, ε_H = Horizontal Strain

ε_a = Axial Strain

ε_{tr} = Transverse Strain

By definition, for a confined linear-elastic and isotropic material, the horizontal stress is a function only of the Poisson's ratio and vertical stress. This relationship can be further expressed as

$$\sigma_H = \left(\frac{\nu}{1-\nu}\right)\left(\sigma_{ob} - P_p\right) + P_p \text{ [13]}, \quad \text{.....(7)}$$

where, σ_H = Horizontal Stress

ν = Poisson's Ratio

P_p = Pore Pressure

σ_{ob} = Overburden Stress

The above expression dictated the relationship between the overburden and horizontal stresses. From the expression, we can easily realized the horizontal stresses will always be less than or equal to the overburden stress when the Poisson's ratio is equal to or less than 0.5. At the same time, this concept provided a base for the prediction of the theoretical fractured plane and its perpendicular nature to the minimum principal stress.

2.4 Fracture Gradient

In order to prevent kicks while drilling it is necessary to maintain a mud weight such that hydrostatic pressure is slightly higher than the formation fluid pressure at any depth. Continuously increasing or decreasing the mud weight enables the drilling operations to overcome possible abnormal and subnormal pressured formations. This however has several consequences, one of which is that increasing mud density might induce an unintentional fracture of the well bore. By the same token, continuously increasing or decreasing drilling mud density will inevitably cause the wellbore to flex and incur additional filtration and mud losses to the formation due to added or subtracted hydrostatic pressure from the mud circulating system. Along with the need to establish the drilling program, casing depth, and mud schedule, it is imperative to determine the fracture gradient for each well.

2.4.1 Fracture Gradient Evaluation

Evaluation of fracture gradient involves evaluating the minimum component of the in situ stresses. Based on the stress concepts, the rock deformation and fracture are controlled by the formation's effective stresses. In theory this relationship is defined as the difference between pore pressure and total stress.

$$\sigma = S - P_p,^{13} \quad \text{.....(8)}$$

where, σ = effective stress

S = total stress

P_p = pore pressure

The theoretical basis for formation fracturing given by Hubbert and Willis[22] stated the total stress is equal to the sum of the formation pressure and the effective stress. The authors gather this conclusion from theoretical and experimental examination of the mechanics of the hydraulic fracturing. The authors suggested that in geological regions where there are not tangential forces, the greatest stress must be approximately vertical and equal to the overburden pressure, while the weaker stress must be horizontal and most likely lies between ½ and 1/3 of the effective overburden pressure. Hence, the overburden pressure (S) is equal to the sum of formation pressure (P_p) and vertical stress (σ_v) effectively supported by the formation matrix. This relationship is illustrated as:

$$S = P_P + \sigma_v, \quad \text{.....(9)}$$

The fracture pressure was then defined by formula as:

$$P_f = \frac{1}{3}(S - P_P) + P_P, \quad \text{.....(10)}$$

Their findings were based on the results of laboratory tri-axial compressional tests. From the experiment, the authors suggested that the pore pressure has no significant effect on the mechanical properties of the rock. However, based on some publications comparing its prediction and actual field data suggested that the results given by it formula are very conservative and limited to specific region.

Matthews and Kelly[23] introduces a variable effective stress coefficient, the formula is then transformed the fracture pressure formula as:

$$P_f = K_i \sigma + P_P \, , \quad \ldots\ldots\ldots\ldots\ldots\ldots\ldots\ldots\ldots\ldots\ldots\ldots\ldots\ldots\ldots\ldots\ldots\ldots\ldots\ldots\ldots\ldots\ldots (11)$$

where, $K_i = \frac{\sigma_h}{\sigma_v}$ effective stress coefficient.

This method is heavily based on empirical data. The values of K_i were dependent on the depth of formation.
The effective stress coefficient described by this method must be validated per local geological information; hence, the effective stress coefficient for the gulf coast may not be suitable for any other geological settings around the world.

Shortly after the publication of Matthews and Kelly's work, Eaton[24,25] stated that rock deformation is elastic, he then replaced effective stress coefficient in the above method by employing Poisson's ratio:

$$P_f = \left(\frac{\nu}{1-\nu} \right) \sigma + P_P \, , \quad \ldots\ldots\ldots\ldots\ldots\ldots\ldots\ldots\ldots\ldots\ldots\ldots\ldots\ldots\ldots\ldots\ldots\ldots\ldots\ldots\ldots (12)$$

On the basis that Poisson's ratio and the overburden gradient vary with depth. Eaton determined values for possion's ratio on the basis of actual regional data for the fracture gradient, the formation pressure gradient and the overburden gradient.

Due to the variability facture gradients from one place to another at identical depth in similar formations, Anderson et *al.* attributed these variations to the shale content of the formations. The relationship was then established between shale content and Poisson's ratio on the basis of Biot's formulation, by Anderson et al.[26]. The shale index is calculated from the log data. It required data from both sonic porosity and density porosity.

$$I_{sh} = \frac{\phi_s - \phi_D}{\phi_s}, \quad \text{.....(13)}$$

where, I_{sh} = shale content index

ϕ_s = sonic porosity

ϕ_D = density porosity

Once the data are available for overburden gradient, sonic and density logs, then the prediction of the fracture gradient can be calculated by Biot's formula or Eaton's method as a simplification. Also, this method only considered predominantly sandy lithologies.

In 1978, Pilkington[27] publicized a method based on a statistical mean of the values of effective stress coefficient and Poisson's ratio by varies authors. Pilkington suggested that the method can be applied to Tertiary basins, such as gulf coast, for both normal and abnormal pressure regimes; however, this method does not apply to brittle rocks. (such as carbonates nor naturally fractured rocks)

Cesaroni et *al.*[28] presented a method that emphasized the mechanical behavior of rocks with respect of fracture gradient. They suggested 3 possible cases: First, he considered the formation had little or no filtrate due to low permeability or rapid mud cake buildup; in this case the differential pressure is almost entirely supported by well bore itself. Hence the fracture pressure is then represented as

$$P_f = \frac{2\nu}{1-\nu}\sigma + P_P, \quad \text{……..(14)}$$

Then, elastic formation with deep mud invasion profile was considered

$$P_f = 2\sigma\nu + P_P, \quad \text{……..(15)}$$

Lastly, for plastic formation

$$P_f = S, \quad \text{……...……...(16)}$$

Breckels and Van Eekelen[29] provide empirical formulations based on the data collected at gulf coast, Brunei and North Sea. The mathematical formula described the relationships between minimum horizontal stress, depth and pore pressure at depth greater than 10,000 ft and less than 10,000 ft. Later, Daines[30] taking up the work from Eaton and introduced a superimposed tectonic stress correction into the fracture pressure calculation. The value for superimposed tectonic stress can be evaluated from the first leak off test of the drilling program. He suggested that this value is constant for the entire well.

2.5 Leak off Test and Formation Integrity Test

To ratify a prediction based on theory, we have to result to an actual field measurement from the formation. The Leak-Off Test (LOT) and Formation Integrity Test (FIT) were introduced to the drilling community. These routine tests are conducted to provide measurements for engineers to determine the feasibility of the mud increase during a drilling program.

A LOT involves pressuring the wellbore utill the exposed formation fractures and or begins to take whole mud. Unlike the LOT, the FIT only involves pressuring the wellbore to a predetermined pressure. Both tests have their place and the decision to fracture the rock depends on such factors as perceived risk, knowledge of the area, and certain aspects of the bore-hole program.[1]

The procedures for the LOT (Figure 2-6) and FIT (Figure 2-7) are similar in concept. Both tests require approximately 10 ft of new formation drilled after drilling out from the shoe. The drilling fluids are then circulated utill it is uniform and clean from drill cuttings. Then the bit is pulled back into the casing, usually a couple of feet. The well is then closed and slow pump rate will then commence the actual test. The pump rate used should be as slow as possible yet must overcome the filtration rate of the fluids. Hence, selection of a casing shoe is a critical task in these types of the operations.

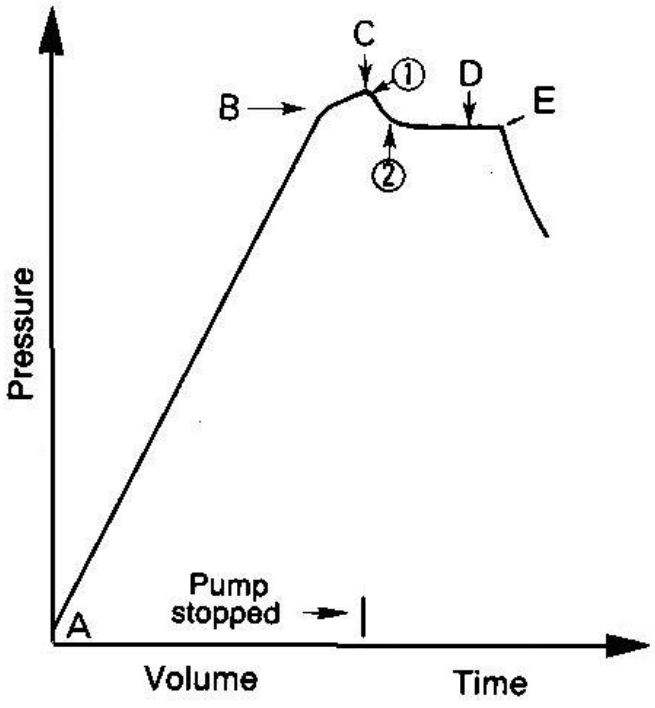

Figure 2-6 Typical LOT Diagram

The Figure 2-6 is typical example of a LOT recording. This can be interpreted as follows:
A-B : linear increase in annular pressure proportional to volume pumped, corresponding to the elastic behavior of the formation.
B : the yield point is reached, formation starts to leak off, this the LOT pressure of the formation
B-C : reduced increase in pressure per volume pumped, mud penetrating the formation.
C : pump stopped. Two scenarios might encounter at this point, either the pressure stabilizes and plateaus (1) or there is a sudden drop in pressure (2) following well breakdown or reopening of a previously created or natural vertical fracture in the well.
C-D : fracture propagation ceases, pressure falls to stabilized pressure regime D which is leas than or equal to pressure at B.
E : end of test, bleed-down the pressure lines.

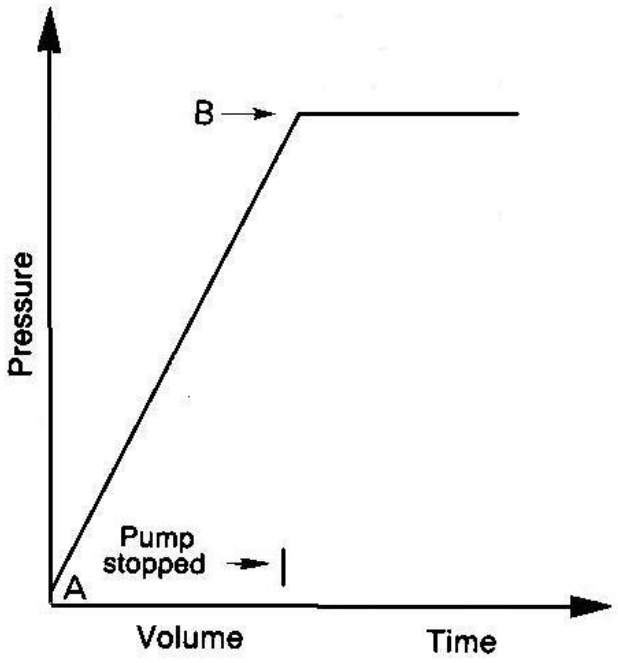

Figure 2-7 Typical FIT Diagram

While the excess pressure is bled-down the amount of mud recovered should be equal to the volume pumped during the actual test. In case the amount of mud recovered will be less than pumped, the pressure at point D is lower than the pressure at point B, it is likely that the cracks will remain partially open, obstructed by cuttings or mud filtrate and prohibiting fluid from traveling back to wellbore. In a permeable zone this may result in major losses of fluids from enlargement of the area of contact between mud and the formation. The LOT therefore runs the risk of weakening the walls of the well bore thus reducing the fracture gradient at this region. In a well known geological area, a predetermined maximum value can be assumed to be sufficient in the light of the expected pressures, so that the formation breakdown pressure is not reached, hence the FIT. However, the values obtained during a FIT test can not be used to evaluate the true fracture gradients of the formation.

2.6 Soil Boring Data

Routine soil boring test were conducted to gather shallow sediment formation information prior a rig being moved to the location. The test would provide the operator with information on sediment weight and density measurements, sediment liquid and plastic limits and sediment shear strength measurements. The Atterberg limits tests were based on Atterberg's [4] possible states of soil; solid, semisolid, plastic and liquid.[2,8,14] These tests are conducted to analyze the possibility of the soil's ability to become a viscous flow by introducing liquidity index. The liquidity index is the ratio of the difference between in situ moisture content and liquid limit and in situ moisture content and plastic limit. If the liquidity index is greater than 1, the sediment could behave with similarity to a viscous fluid. The sediment shear strength measurements can provide information necessary to perform the Skempton calculation.[2] Skempton's method was based on an empirical relation between shear strength and vertical effective stress for normally consolidated sediments. The Skempton formula shown as:

$$\frac{C_u}{\sigma_z} = 0.11 + 0.0037(L_l - P_L), \quad \text{……(17)}$$

where, C_u = undrained shear strength

σ_z = vertical effective stress

L_l = liquid limit

P_l = plastic limit.

With this correlation it is then possible to estimate the vertical effective stress for the shallow sediment within the normally consolidated formation, especially in the shallow marine depositional environment.

3 RISK ASSESSMENT AND EVALUATION

Engineering practice developed over the years combined both past experiences, theories and technologies of past, present and future. These engineering practices were the foundation of today's industry standards along with design and operating practices. In the most part, the processes generate results based on levels of reliability which the standards and practices have incorporated. Hence, objects have designed and implemented with engineer explicitly choosing any reliability level or any risk analysis. Even when reliability is considered for E&P industry operations, the calculation of risk has usually been based only on a subjective consideration of the consequences of failure.

3.1 Risk and Uncertainty

Risk contained the two notions of probability of an undesired event occurring and the severity of the consequence. This can be easily recognized by a mathematical relationship as:

$$\text{Risk} = \text{Probability} \times \text{Consequence}$$

With the help of a mathematical expression, the risk is still difficult to analyze. This is partially contributed by the fact of determination of reliability.[31,32,33] In general, it is the role of the scientific professional to determine reliability, whereas other factors in the surrounding society determine the acceptable level of risk. Hence, it is imperative that engineers design systems which meet the expectations of their societies with regard to risk.

3.1.1 The Monte Carlo Method

This mathematical method is used by the commercial software packages, such as "Crystal Ball" and "@RISK". The method is ideally suited to computers as the description of the method have revealed.

The Monte Carlo simulation is generating a limited number of possible combinations of variables which approximates a distribution of all possible combinations. The more sets of combinations presented, the closer the Monte Carlo result will be to the theoretical result of using every possible combination. If two variables are dependent, then the value chosen in the simulation for the dependent variable can be linked to the randomly selected value of the first variable using the defined correlation.

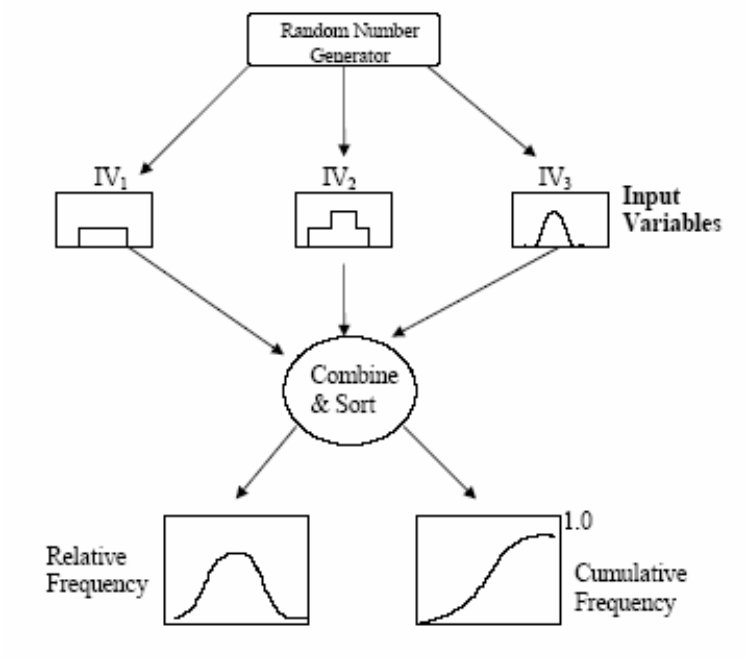

Figure 3-1 Typical Monte Carlo Flow Chart

Monte Carlo simulation takes advantage of the computer, it's fast, and the presentation of the simulated results usually are attractive to management. However, the repeatability of the result with the same input variables is very liberal, making the result less auditable.

But on the other hand, more simulation runs can reduce the uncertainty of the result and increase repeatability. This method uses coefficients to overcome the lack of ability in sensitivity analysis. Figure 3-1, shown above detailed a typical Monte Carlo computational flow chart.

3.1.2 The Parametric Method

The parametric method is an established statistical technique used for combining variables containing uncertainties and has been utilized within the drilling community. HAZOP is one of the examples of the parametric method. The main advantages of the method are the simplicity and it's ability to identify the sensitivity of the results to the input variables. This allows a ranking of the variables in terms of their impact on the uncertainty of the result. At the same time indicates where effort should be directed to better understand or manage the key variables in order to intervene and mitigate downside, and or take advantage of upside scenarios. The method allows variables to be added or multiplied using basic statistical rules and can be applied to dependent as well as independent variables. If there is insufficient data to describe a continuous probability distribution for a variable, then a subjective estimate of high, medium and low values can be employed. Figure 3-2, details a typical parametric method.

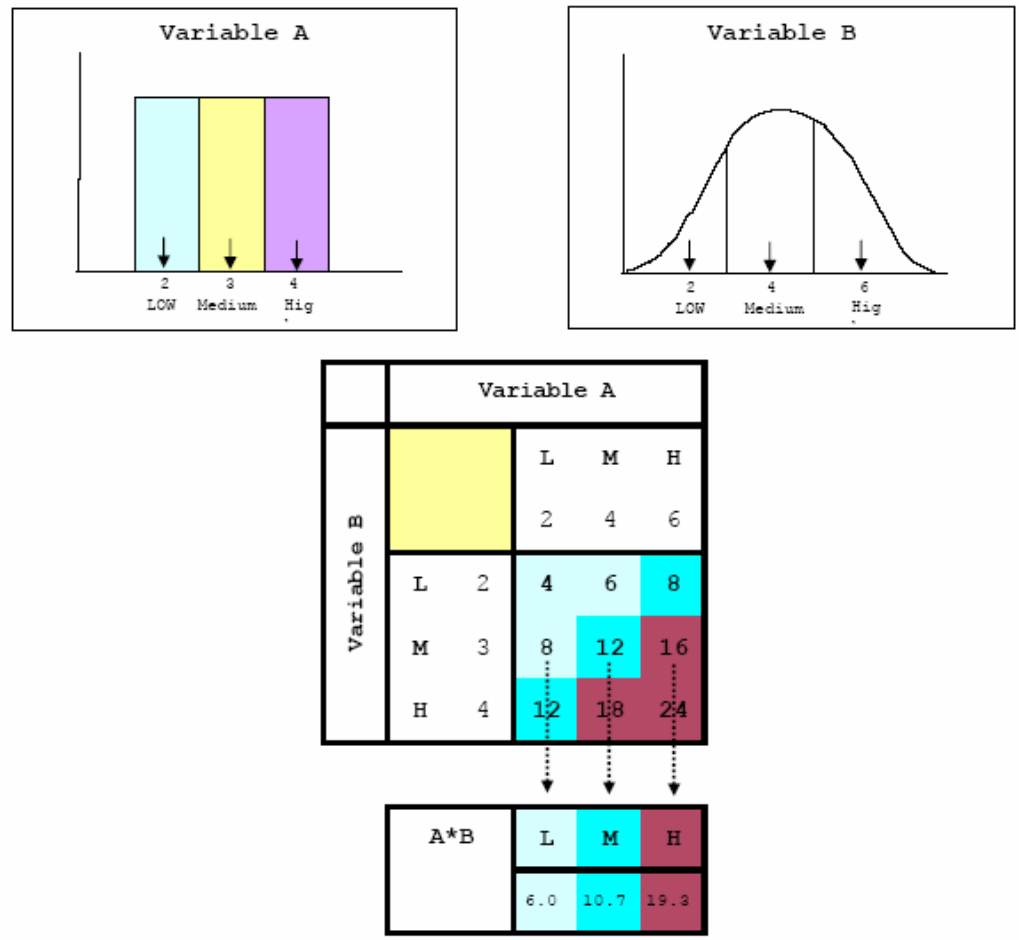

Figure 3-2 Typical Parametric Method Flow Model

3.2 Methods for Conductor Setting Depth Evaluation

Techniques for predicting, estimating and detecting abnormal formation pressure can be classified as:

- Predictive methods
- Methods applicable during drilling operation
- Verification methods

Initial well planning of a rank wildcat well must be based on formation pressure information obtained by a predictive method. The initial estimates will be updated continuously during the drilling operation with additional available information. After reaching total depth of section or a well, the formation pressure estimates are again checked, using various formation evaluation methods, such as electric logs, formation pressure test data, etc.

3.2.1 Predictive Methods

Predictive methods involve obtaining information from previously drilled wells with similar geological characteristics to the current objective. The physical basis for the determination of porosity and pore pressures from seismic measurements has been the often-observed correlation between seismic velocity and porosity and between porosity and effective pressure.[35] Formation porosity and compaction can be derived from actual subsurface measurements, such as resistivity logs, sonic logs, etc. Drilling conditions from mud logs, and bit records from a near by field can also be useful to predict the pressure and compaction trends. In any case, the best results are obtained when the well planner is able to obtain information from a variety of sources.

Care should be taken when using mud and bit records because they are often inaccurate or sometime misleading. First make sure that the data are from the same geological sequence. In many areas, especially in areas of dense faulting, there can be great differences in pore pressure at the same depth over relatively short horizontal distances.

Once satisfied with reasonably accurate records, one can predict pore pressures by correcting the reported mud weights for swab pressure; i.e., mud weight should be 0.3 ppg higher than pore pressure to control swabbing when making a trip. Even though written records do not usually give pinpoint accuracy in estimating pore pressures, they

are useful in constructing at least a qualitative pressure profile. They can point out the likely existence of a transition zone as well as some indication of its location.

3.2.2 Methods Applicable While Drilling

Since the formation pressures is seldom read directly but is determined from other parameters. One of the parameters frequently used is effective stress, since effective stress and pore pressure are directly related as the two components of total pressure. Effective stress is overcome many times while drilling by the action of the drill bit. This makes the drill bit an excellent sensor. As we know, as the pore pressure increases, the effective stress decreases. So everything else being constant, the drilling rate will increase. Several empirical relationship, such as the “d” exponent, have been developed which permit the calculation of formation pore pressure in terms of normalized drilling parameters. Most mud logging service providers offer plots of pore pressure based on some combination of drilling parameters as part of their standard service.

Drilling rate is also effected by the relationship of borehole pressure to formation pore pressure. The greater the value of formation pore pressure compared to borehole pressure, the greater the drilling rate. This is due to the fact that shear strength of sediments are directly related to their confining pressure. As sediments are exposed to the borehole, their confining pressures are either increased or reduced according to the borehole pressure. If the mud in the borehole exerts a pressure that is greater than the pore pressure, then the confining pressure on the formation is increased and so is it's shear strength. Conversely, if borehole pressure is less than formation pore pressure, confining pressure is reduced and so is the shear strength. Since drilling rate varies with shear strength of the sediments penetrated and since borehole pressure is a known quantity, then pore pressure can be determined from variances in drilling rate.

Current Logging While Drilling (LWD) and Measurement While Drilling (MWD) technologies have placed great emphasis on Pressure While Drilling (PWD) measurements. Tools such as the Annular Pressure While Drilling (APWD), developed by Schlumberger, can provide direct pressure and temperature measurements in the subsurface environment while drilling. These measurements are then transferred via a mud-pulsing telemetry system through the mud column and deliver the pressure data to the operator. In most of cases, these measurements were presented as Equivalent Circulating Density (ECD). Combining this data with resistivity log data, sonic shear and or compression data and conventional mud logging services, a pore pressure technician can provide a reasonable estimate of the actual pore pressure trend.

3.2.3 Verification Methods

By definition, verification methods are after-the-fact methods. After a well has reached its total depth, particularly if it is completed for production or a wireline formation evaluation tool has been run, the well planner has as good information about the formation as it is possible to get. However, in real life, once the drilling operation is completed and the urgency of knowing or estimating pore pressure is not so acute; data are ignored and archived in their raw state. The planner of the next well is usually faced with the same task of gathering raw data and making his/her own determinations rather than being supplied with an analysis that would provide conclusive information. Hence the best time to analyze data is when they were being collected and generated.

4 DISCUSSION AND CONCLUSION

4.1 Discussion

4.1.1 Seismic

Present day methods of exploiting seismic data can provide numerous clues for detecting abnormally pressured zones, as well as geological information, such as

- The approximate lithologies and facies of the geological sequence
- Direct hydrocarbon detection, i.e. Bright Spot Analysis
- Prediction of abnormal pressure tops and quantitative pressure evaluation
- High resolution, shallow depth investigation and disclosure of shallow hazards.

Techniques such as “Very High resolution seismic” can be carried out for the study of seabed. It has a resolving power down to less than 3 feet, and its depth of investigation is limited to 150 to 300 feet. This technique has been widely used for platform anchorage and can also provide the driller with a shallow geo-hazard prognosis close to seafloor. Individual service providers can provide the operator with the seismic data along with a detailed shallow hazard analysis report.

The “High resolution seismic” technique has a resolution in 3-15 feet range and a depth of investigation reaching between 3,000 to 5,000 feet. This technique is commonly used in conjunction with conventional seismic methods.

The traditional seismic technique has a lower resolution, in the 15-150 feet range, but a depth of investigation extending to several thousands of feet. It is the most important source of information about abnormally pressured zones in the vicinity of planned well bore. The traditional way of representing transit times is by means of a seismic section, a method based on seismic reflections. Sometimes it is also possible to ascertain the

different sequences of sedimentation by breaking the image down into sequences of seismic wave trains. This can give useful information about the sedimentation pattern.

The interval velocities of the seismic data can be used when the structures are not complex and the series is sufficiently thick, and it is possible to evaluate transit times and calculate the propagation velocity for each interval in the formation.

4.1.2 Predrill Estimation

Most predrill estimations are based on the assumption of the formation has not been subjected to any lateral deformation since sedimentation and that is always deformed elastically during compaction. Hence the physical measurement itself and the method provided by the authors mentioned in previous sections include isotropic Poisson's ratio for direct estimation of in situ stresses. Therefore the utilization of the coefficient for the effective stresses based on an isotropic Poisson's ratio must be carefully considered prior to applying to the aforementioned methods, such as Hubbert and Willis[22], Eaton[24,25] and etc.

The study carried out by Mukerji *et al*[12] concluded that the geophysical basis for the determinations of porosity and pore pressures from seismic measurements; correlations between seismic velocity and porosity and between porosity and effective pressure has been the often-observed. Based on theory, geopressure implies low effective stresses and increased porosity, which in turn have a pronounced effect on the geophysical properties such as seismic velocity, formation density, formation electrical conductivity and strength, especially in soft or unconsolidated sediments. They concluded the ratio between velocity of P-waves and velocity of S-waves is one of the critical seismic signatures that can detect low effective pressure, and consequently provide us with this general equation for an in situ Poisson’s ratio estimation:

$$\nu = 0.5\frac{\left(\frac{V_P^2}{V_S^2} - 2\right)}{\left(\frac{V_P^2}{V_S^2} - 1\right)}, \quad \text{.....(18)}$$

where, υ = Poisson's Ratio

V_p = Velocity of P-Wave

V_s = Velocity of S-Wave

This method would greatly increase the confidence in the estimation of Poisson's ratio for a given location.

4.1.3 LOT and Soil Boring

As indicated in section 3, formation pressures are seldom read directly but are determined from many parameters. Some of the conventional drilling and formation evaluation methods have been compromised in the recent years; control drilling technique is used to overcome low narrow pressure window of the well profile and utilization of LWD and MWD tool was almost eliminated in the large borehole sections purely due to the tool's lack of depth of investigation. However, pressure related measurements, such as PWD, LOT and Soil Boring techniques can be utilized in examining the formation pressures.

In the soil boring data gathered by Wojtanowicz *et al.* [2] for the Green Canyon area of GOM; the sediments collected were impermeable and plastic in nature. The sediment is composed mostly of clay and classified as very soft to soft. The ratio between horizontal to vertical effective stresses was near 1.0 over the entire interval. A sediment bulk density vs. depth (datum = sea level) chart for this region was presented. (Figure 4-1)

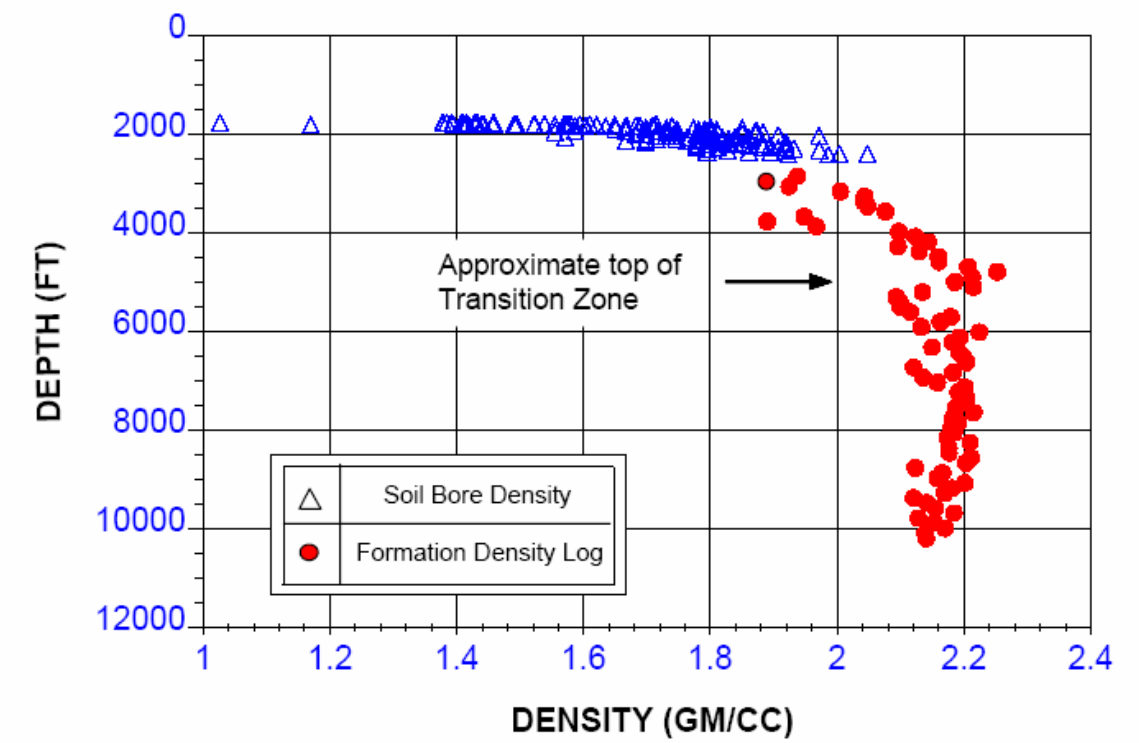

Figure 4-1 Sediment Bulk Density vs. Depth in Green Canyon, GOM[2]

The LOT data obtained and subsequently analyzed by the group indicated the onset of formation breakdown can't be clearly identified in a soft formation. This phenomenon can be illustrated as below, by comparing a LOT performed in a deeper formation thus has an elastic-plastic behavior (Figure 4-2) with a LOT performed in shallower formation with a non-linear elastic behavior (Figure 4-3). For a non-linear elastic formation, it is widely believed that the weakest point in a wellbore is the shoe. This could partly due to pre-existing “cement channels” in the cement bonding with the casing and actual formation. These cement channels could provide the necessary pathway for the drilling fluids to be leaked off to a shallow and/or more permeable formation.

When comparing a deep LOT with a shallow LOT, the results usually may cause the operator to felt less certain about performing a LOT in the shallow marine sediments.

The potential of unwillingly damaging the formation, weaken the formation integrity and/or induce a pre-existing cement channel to facture have virtually eliminated LOTs in the shallow marine environment.

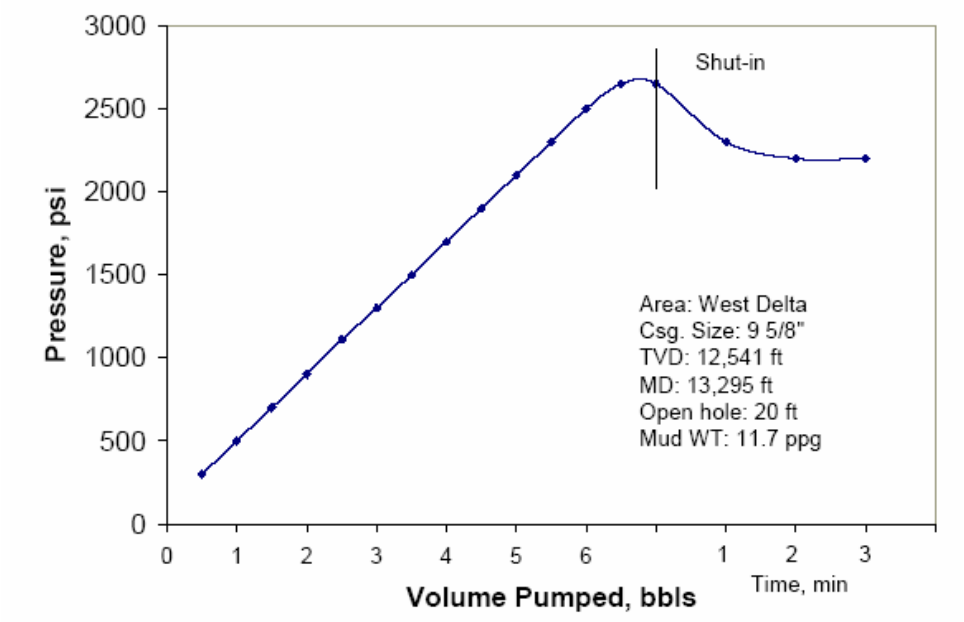

Figure 4-2 Typical Elastic-Plastic Deep Formation, LOT [2]

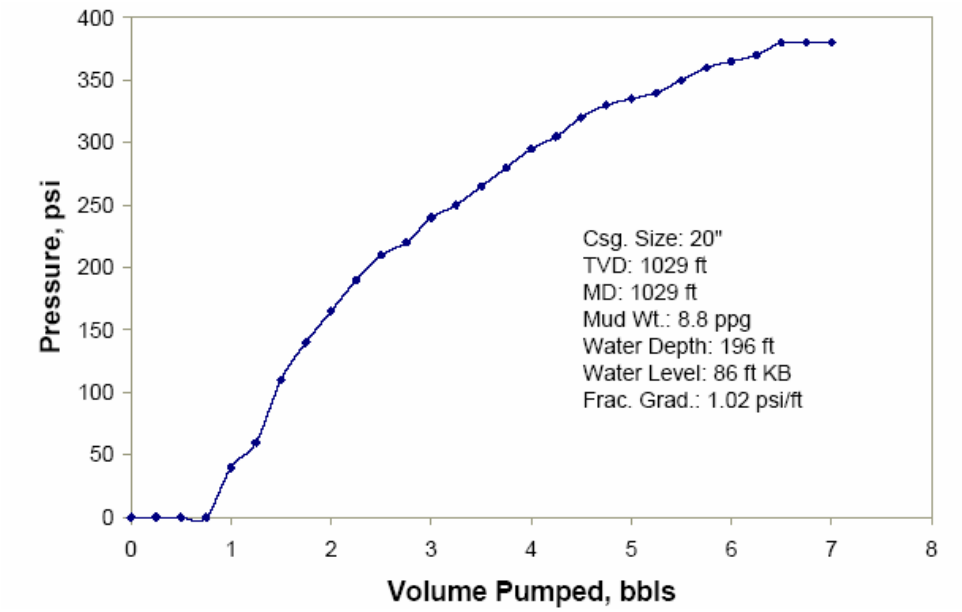

Figure 4-3 Non-linear LOT in SMS[2]

In the same study, the LOT was plotted against depth, within its perspective geological settings; such as the High Island area of the GOM (Figure 4-4). The analysis presented by the paper show a large data scatter in all drilling areas considered. Only the deeper portions of the LOTs did the data correlate. The LOT data (Figure 4-5) from the North Sea region behaved similarly to the data from GOM.

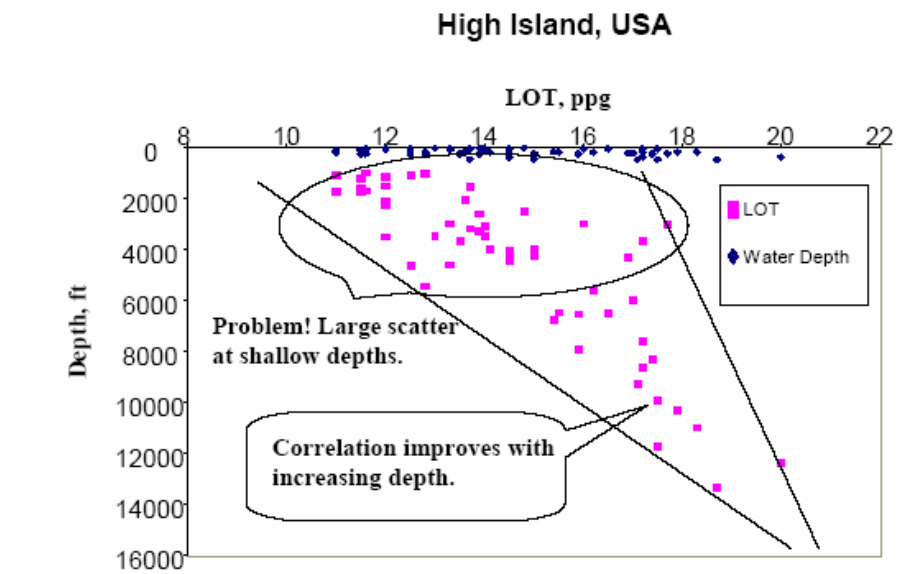

Figure 4-4 LOT Data Scatter with Depth, High Island, GOM [2]

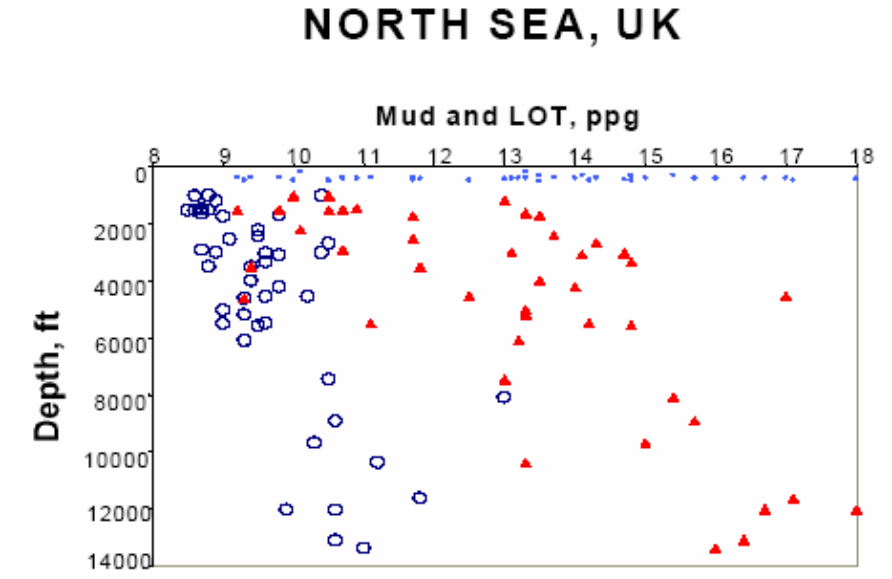

Figure 4-5 LOT from North Sea, UK, Shown No Correlation [2]

4.1.4 Conductor Setting Depth Evaluation

The concepts of horizontal and vertical stresses were first introduced in section 2.3.3 along with a mathematical expression displayed the relationship between the horizontal stress, pore pressure and overburden stress. The expression (Eq.7) provided insight on the dependency and controlling factors within the relationship.

Figure 4-6 displays pore-pressure, constant overburden stress and horizontal stress for a formation with constant rock properties. With respect to this hypothetical case, the overburden stress was greater than horizontal stress at all depths; therefore vertical fracture path can be predicted for all depth.

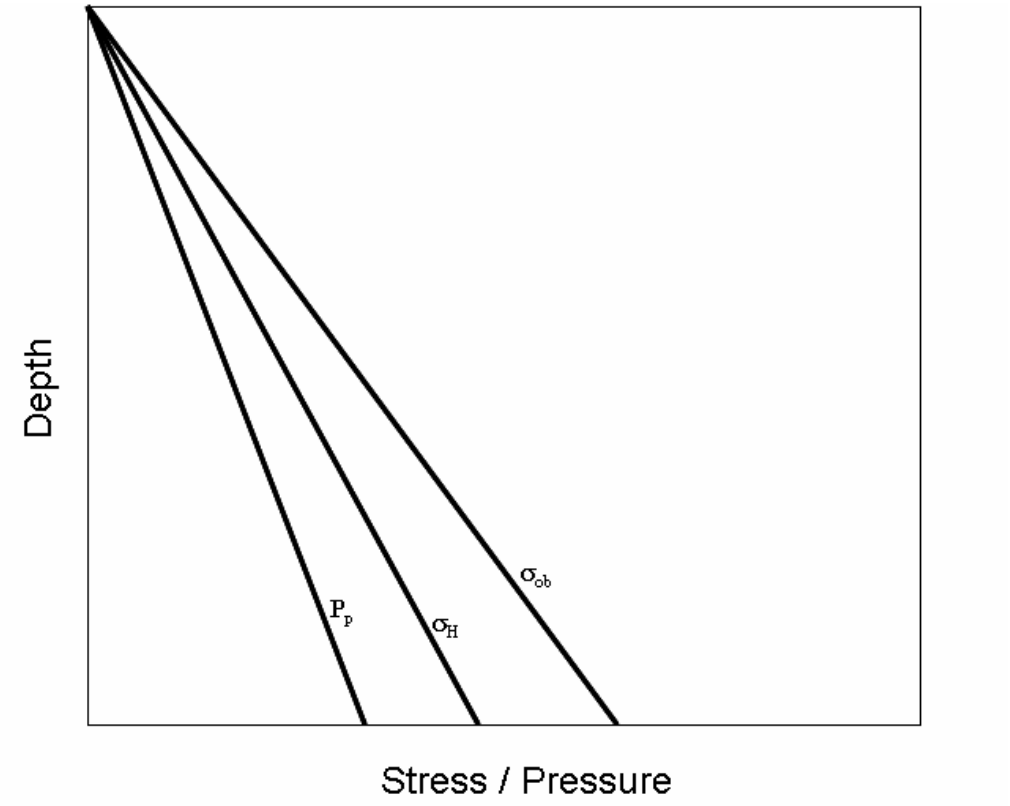

Figure 4-6 Horizontal Stress, Pore-Pressure, and Overburden Stress Diagram for Constant Rock Properties[13]

As discussed in section 2.1.1, bulk density and overburden pressure increases with a reduction of formation porosity. It is conceivable, along with a constant pore pressure gradient, the increase in overburden pressure would ultimately lead to a reduction in horizontal stress. This can be ratified by utilizing the horizontal stress relationship described in section 2.3.3.

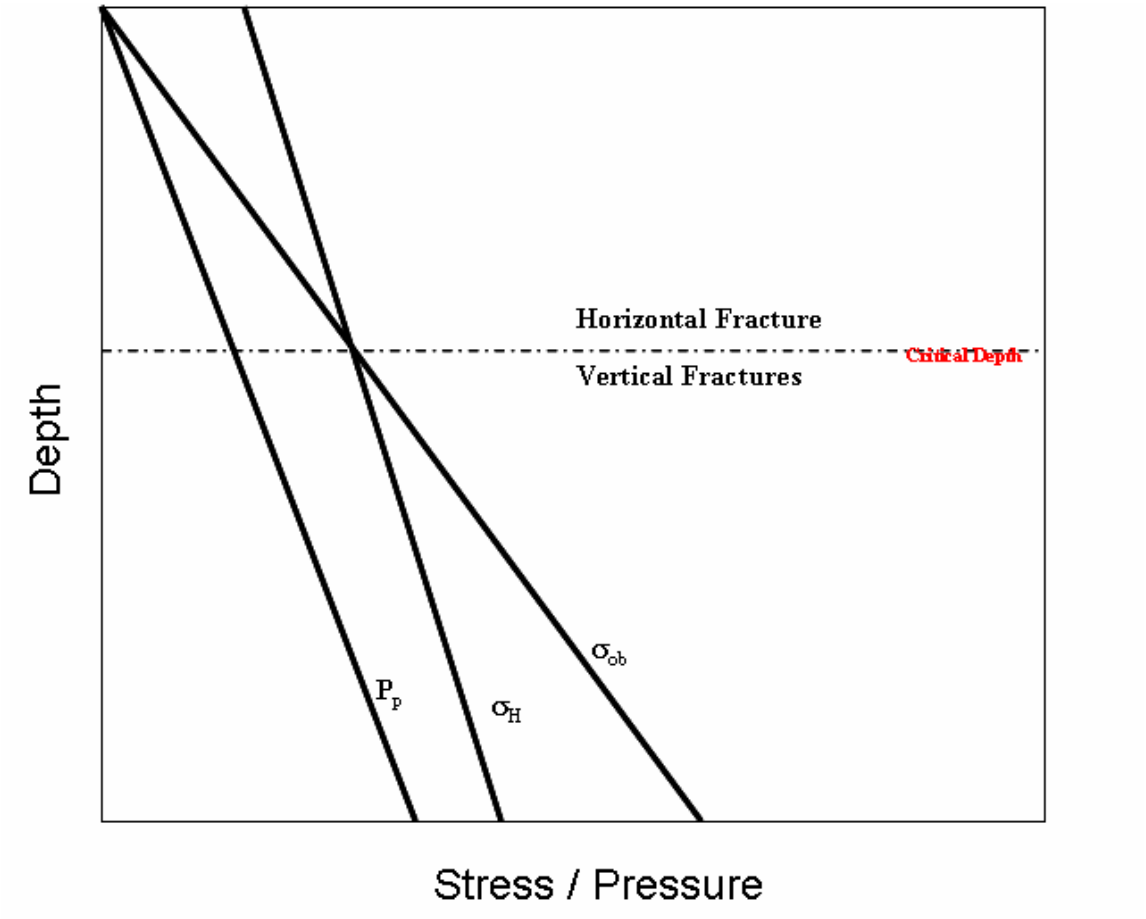

Figure 4-7 Conductor Setting Depth, Critical Depth[13]

Figure 4-7, illustrates the concept of critical depth where the transition of horizontal fracture pattern and vertical fracture pattern within the shallow strata. The figure also suggests, a non-linear elastic behavior LOT is likely associated with horizontal fracture

patterns and linear elastic-plastic behavior LOT can be associated with vertical fracture patterns.

The concept of critical depth for facture patterns can be further utilized for the proper identification of well control equipment and methods. If the conductor casing shoe depth is above the critical depth, then the consideration of likelihood of formation fluids broaching to surface in a non-linear elastic shallow formation via cement channels should be considered as a possibility of well control events.

To determine the fracturing pattern for a given shallow formation the bulk density must be determined. The bulk density can be measured directly from the soil boring samples taken at the shallow depth and use the overburden gradient approximation at greater depth. The overburden pressure gradient can be derived directly from the soil boring bulk density. The measured overburden gradient from soil boring is

$$g_{ob}\left(\frac{psi}{ft}\right)=\frac{\rho_b\left(\frac{lbm}{gal}\right)}{19.25}, \quad \text{.....(19)}$$

and the Mitchell's[13] overburden approximation for deeper sediments

$$g_{ob}=0.84753+0.01494\frac{D_{se}}{1000}-0.0006\left(\frac{D_{se}}{1000}\right)^2+1.199\times10^{-5}\left(\frac{D_{se}}{1000}\right)^3, \quad \text{.....(20)}$$

can be utilized as an approximation, where direct soil strength measurement is not possible.

By definition, the overburden stress is equal to the overburden pressure gradient multiplied with the corresponding depth. Use a linear interpolation method between the

end of the measured overburden stress and beginning of the overburden polynomial approximation for the entire formation.

The impact of water depth and air gap just below the rig floor on the fracture gradient must be carefully considered for a shallow water drilling project. This is due to the significant impact of water depth and air gap on the fracture gradient in the case of the bottom supported rig in shallow water environment as compared with land operations. Figure 4-8 shows depth components imposed on the overburden gradient for both land and shallow water drilling operation. For the land rig, one of the contributors is the sediment depth, $D_{s,}$ and another is the air gap between the Rotary Kelly Bushing (RKB) and ground. For the shallow water rig operation,

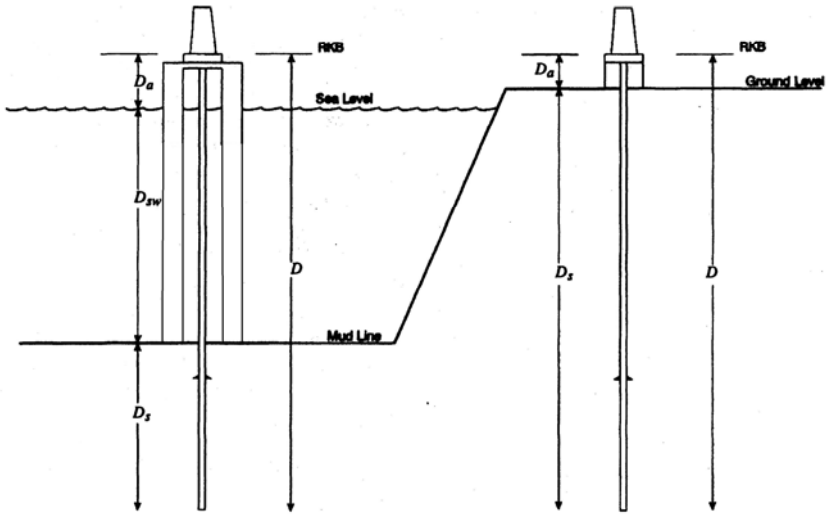

Figure 4-8 Overburden Stress Components for both Bottom Supported Rig and Land Rig

overburden gradient contributors such as air gap (D_a) between the water and RKB, the water depth (D_{sw}) and sediment depth (D_s) must be considered for the evaluation of the fracture gradient.

The pressure gradient for sea water and the air gap can be calcuated as below; all pressure and/or stress calculations should consider same datum point at RKB.

$$g_{sw+air} = \frac{0.052 * D_{sw} * \rho_{sw} + 0.052 * D_a * \rho_{air}}{D_{sw} + D_a}, \quad \text{.....(21)}$$

where, g_{sw+air} = pressure gradient, seawater and air gap

ρ_{sw} = density, seawater

ρ_{air} = density, air

D_a = depth, air gap

Dsw = depth, seawater

An approximation between sediment depth and water depth can be realized by comparing the density of sea water, 8.6 lbm/gal, and typical formation density between 16 lb_m/gal to 20 lb_m/gal. Assuming air density is relatively small compared with the sea water density and formation density.

$$D_{s(eq)} \approx \frac{D_{sw}}{2}, \quad \text{……(22)}$$

where, $D_{s(eq)}$ = Equivalent-sediment Depth

and effective sediment depth

$$D_{se} = D_{s(eq)} + D_s, \quad \text{……..(23)}$$

where, D_{se} = Effective Sediment Depth

D_s = Sediment Depth

The effective sediment depth should be utilized when estimating depth related stresses and pressures. Based on seismic data, Poisson's ratio can be calculated by utilizing Eq.

18. The horizontal stress then can be calculated with Eq. 7 discussed earlier in section 2.3.3.

4.1.5 Data Analysis and Results Discussion

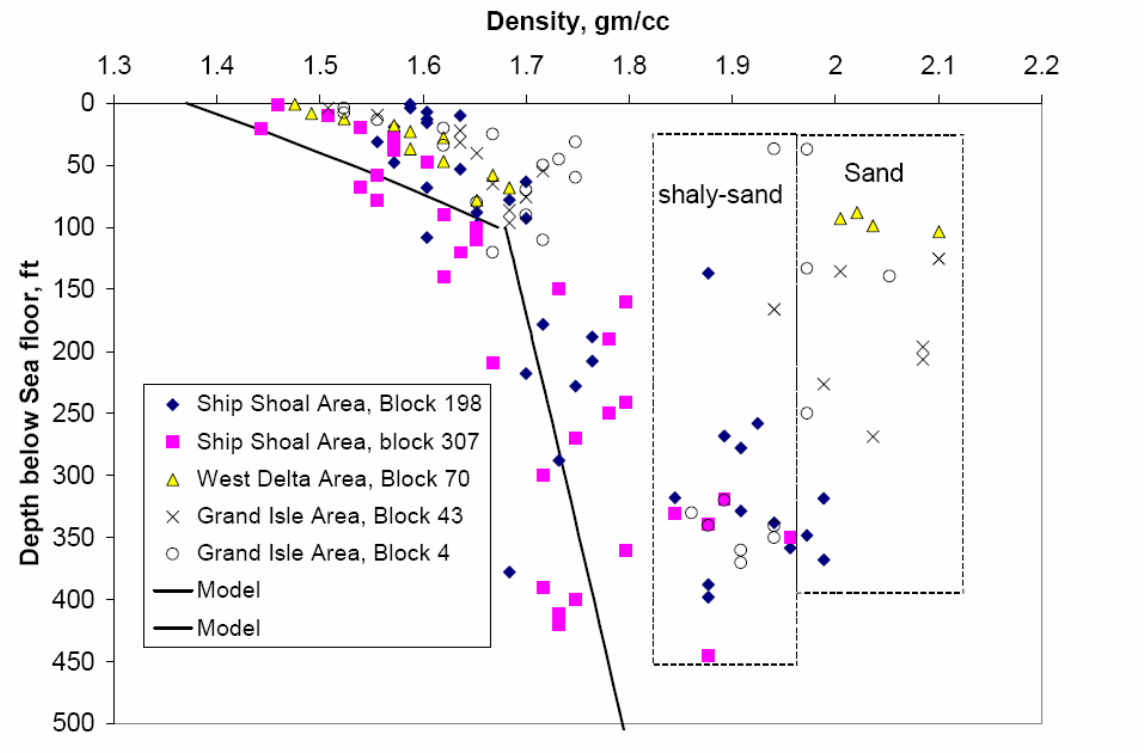

Figure 4-9 Density of Sediments in SMS, GOM[2]

Figure 4-9 shows density data from five different locations taken west of the Mississippi Delta, near the Louisianan coast line, central Gulf of Mexico. (See Figure 4-10)

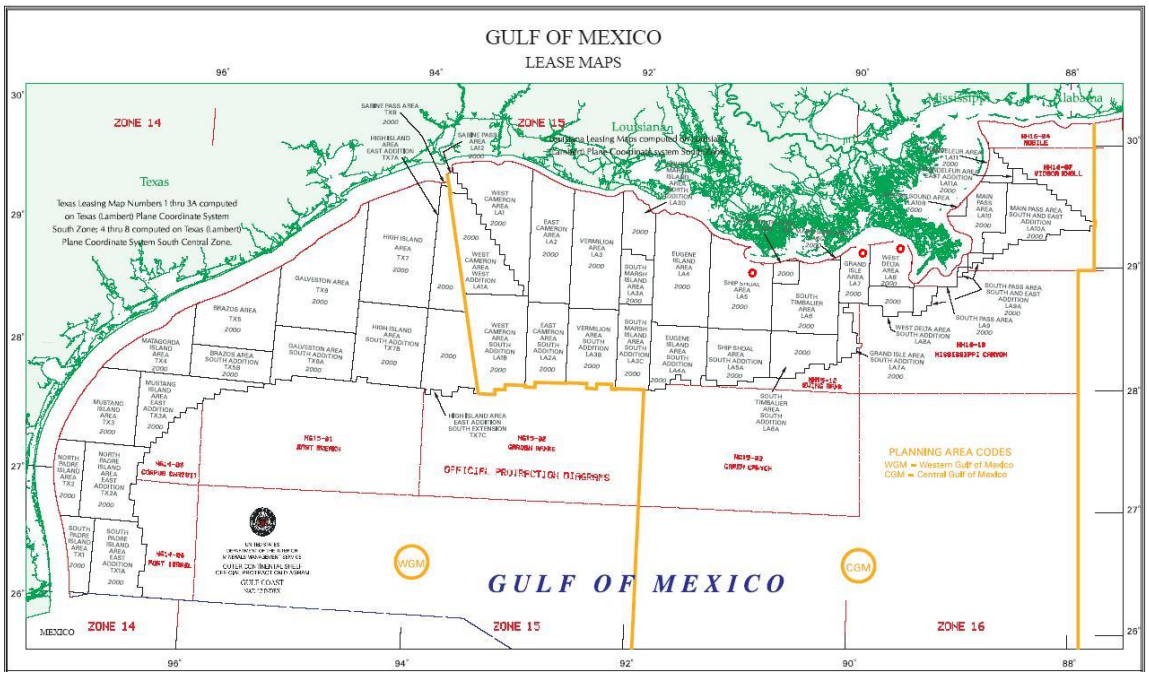

Figure 4-10 Gulf of Mexico Lease Maps, MMS

The data were first extracted by a digitizer; individual area data sets were generated. Based on the method indicated in the previous section, the data sets were then carefully analyzed and calculations were made to generate the overburden stresses, horizontal stresses, and pore-pressures for each of the five areas for comparisons. Graphic representations were generated to indicate trend lines of the formation pressures and stresses vs. depth below mudline.

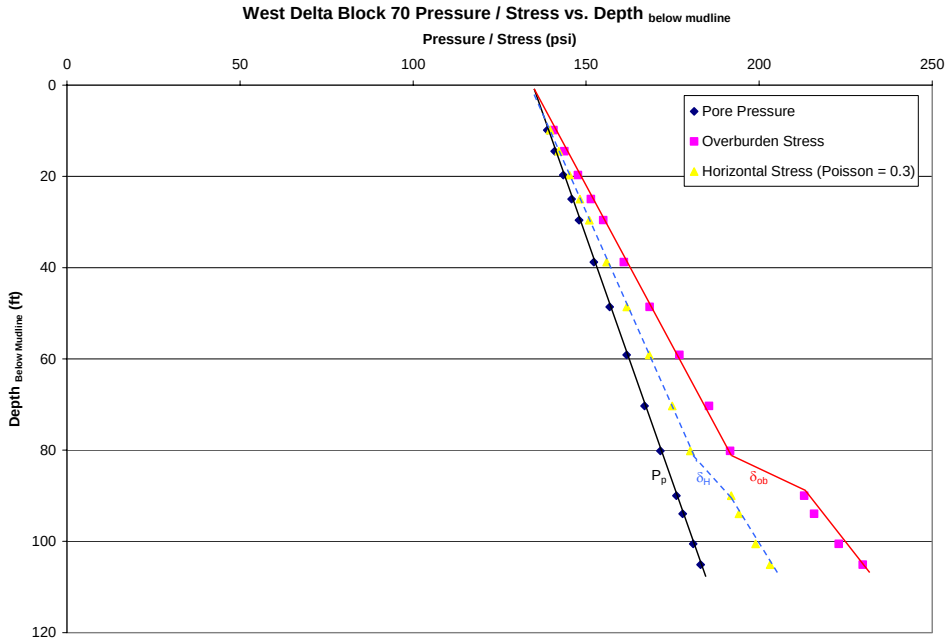

Figure 4-11 West Delta Block 70, Pressure / Stress vs. Depth below mudline

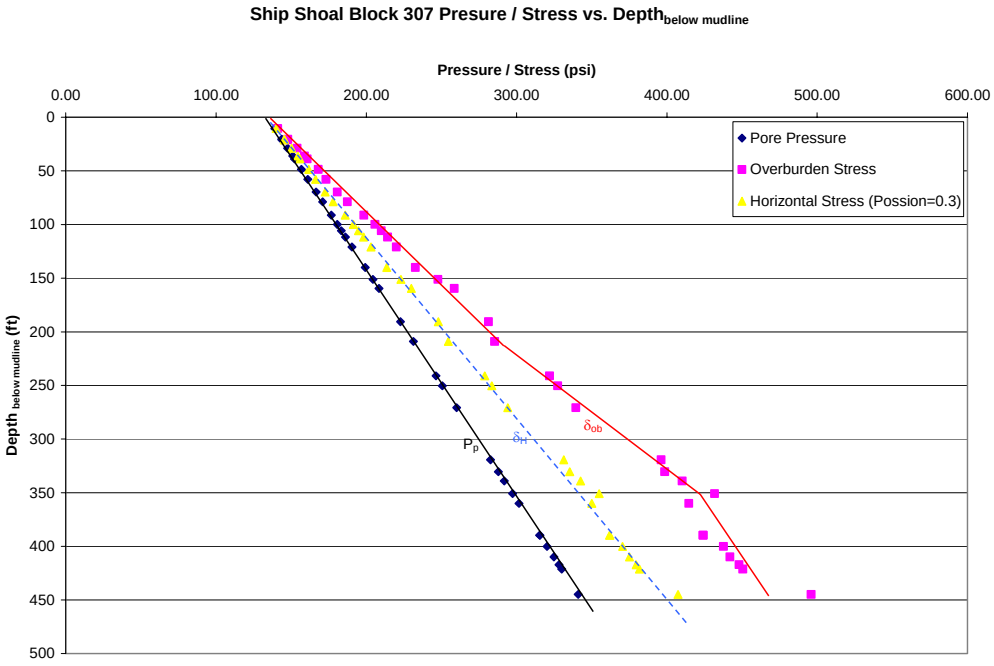

Figure 4-12 Ship Shoal Block 307, Pressure / Stress vs. Depth below mudline

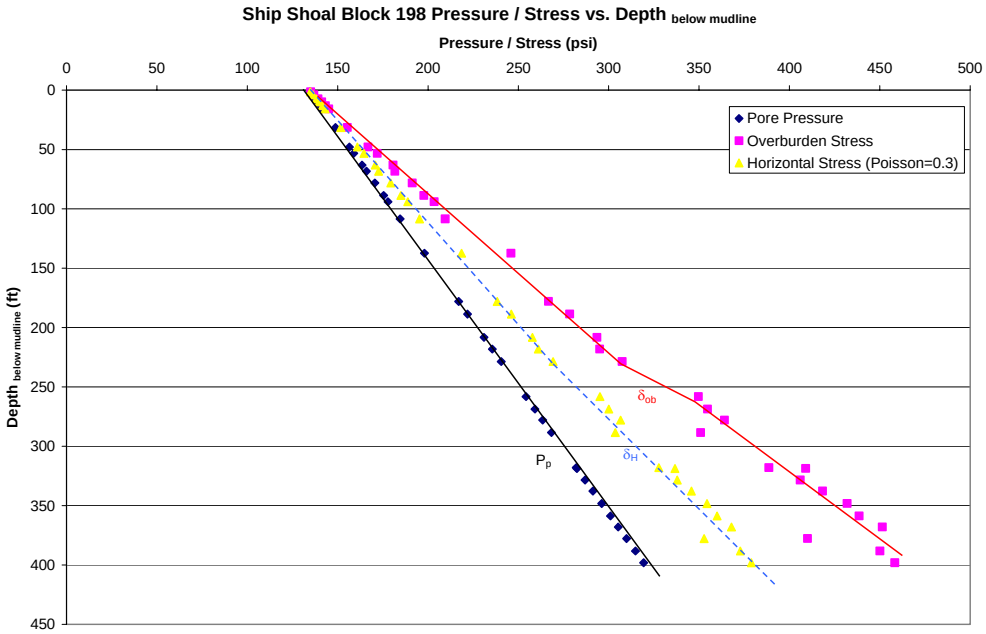

Figure 4-13 Ship Shoal Block 198, Pressure / Stress vs. Depth below mudline

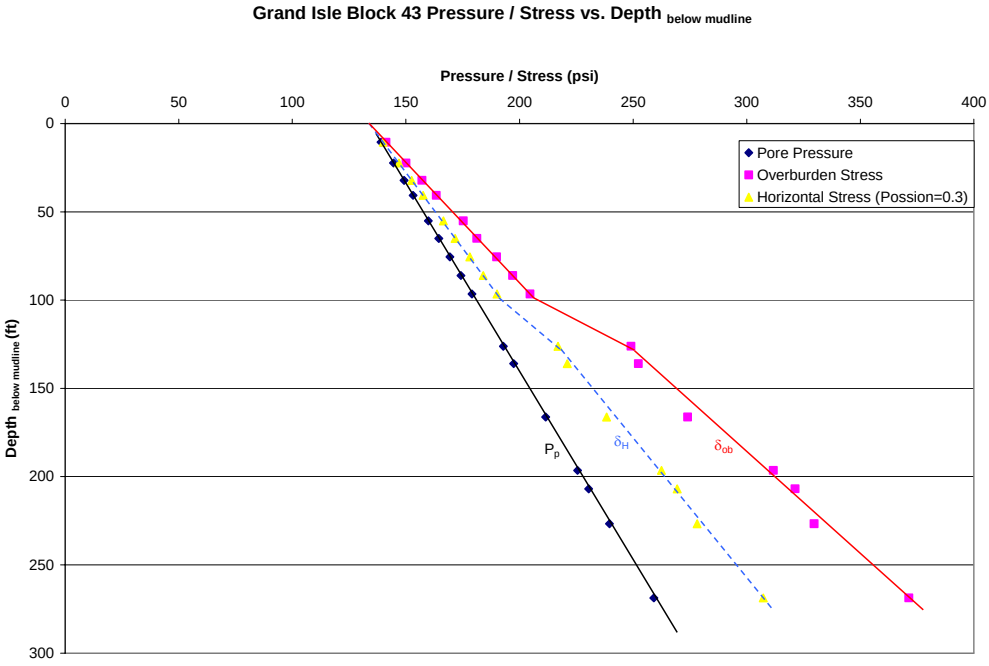

Figure 4-14 Grand Isle Block 43, Pressure / Stress vs. Depth below mudline

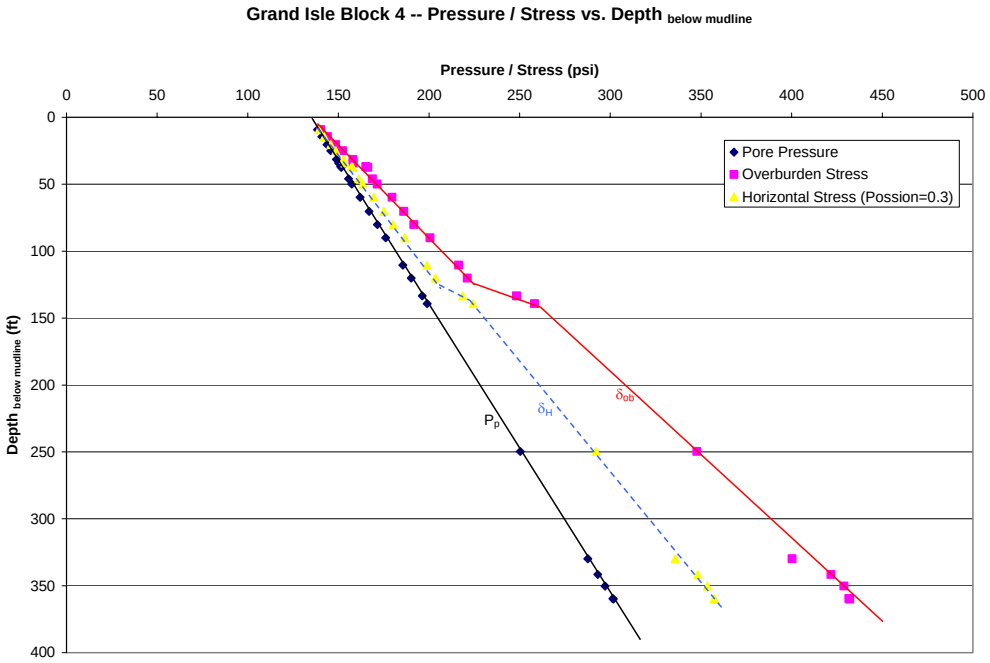

Figure 4-15 Grand Isle Block 4, Pressure / Stress vs. Depth $_{\text{below mudline}}$

The Overburden Stresses (δ_{ob}) were calculated based on the measured soil boring data for each of the locations. The assumed normal pore pressure gradient (0.465 psi/ft) were used to estimate the Pore Pressures (P_p) for each given depths. The assumed 0.3 Poisson's ratio[13] was utilized to calculate the Horizontal Stresses (δ_H) for corresponding depths. For detailed calculation procedure and results, see Appendix A.

Over all, the horizontal fractures were nonexistent for the data sets. (Figures 4-11 to 4-15) Furthermore, based upon the calculations all locations presented with vertical fracture tendencies only.

Geological transitions were detected at the depth between 100 ft to 150 ft and 200 ft to 250 ft below mudline, based on the Overburden Stresses trend lines, for the Grand Isle Blocks and Ship Shoal Blocks respectively.

4.2 Conclusion

In conclusion, soil boring measurements and interpretation of the data should provide operators with an effective means of formation pressure and stress prediction in the SMS environments of the GOM. All calculations for pressure and or stress must have a common reference point, such as RKB. The seismic data, when available, should be used in conjunction with soil boring data for generating the Poisson's ratio and estimating pore-pressure in the SMS of the GOM; hence a better analysis can be made using mathematical relationship, such as Eq. 7. The critical depth concept along with operational considerations and engineering economics should be the key elements for the selection of the conductor setting depth in the shallow water of GOM and well control contingency plans; however, none of the data sets gathered for this study indicated a horizontal fracture patterns. The LOT data scatter effect (Figure 4-4 and Figure 4-5) along with formation pressure and or stress analyses indicated strong influences of the regional geological settings.

Furthermore, the results from this study provided the validity required for the rejection of the "rule of the thumb" methodology for the conductor setting depth and provide feasible engineering theories and calculation approach for the conductor setting depth estimation in terms of pressure and stress predictions.

For the well control contingency and based upon the results of study; a Blowout Preventer (BOP) with the ability to divert formation fluids at surface should be considered when drilling the open-hole of the conductor section. The suggestion of the equipment was due to its ability to shut-in wells, the expandability of linear elastic-plastic formation and previous casing shoe to withstand formation influx during an actual well control event. To be able to shut-in a well and circulate the kick out of hole, the well control team must have knowledge of maximum yield point of the formation and integrity of the pervious casing shoe. In the event, the formation influx is greater than the maximum yield point obtained during the pervious LOT; the entire system

should be then placed on the diverter system as primary well control method and provide crucial time required for proper well control actions.

4.3 Future Work

Future study should expand on current drilling guidelines from industry leaders and text books, to evaluate the conductor setting depth criteria, and to develop a guideline for the shallow hazardous formations. The study should also include the need for the ability to shut-in on conductor casing in well control situations, as well as the need to pressure test the conductor-casing seat.

NOMENCLATURE

A	=	area, ft^2
APWD	=	annular pressure while drilling
C_u	=	undrained shear strength, psi
D	=	vertical thickness of the overlying sediments, ft
D_a	=	air gap, between the RKB to sea level, ft
D_s	=	sediment depth, ft
D_{se}	=	effective sediment depth, ft
D_{sw}	=	water depth, ft
E	=	young's modulus
ECD	=	equivalent circulating density
F	=	force, lb_f
FIT	=	formation integrity test
g	=	acceleration of gravity, 32.17 ft/s^2
g_{ob}	=	pressure gradient, overburden, psi/ft
$g_{sw+aire}$	=	pressure gradient, seawater and air gap, psi/ft
GOM	=	Gulf of Mexico
h	=	vertical height of the fluid column, ft
I_{sh}	=	shale index, dimensionless
JIP	=	joint industry project
K_i	=	effective stress coefficient, dimensionless
L_l	=	liquid limit
LOT	=	leak-off test
LWD	=	logging while drilling
MMS	=	Mineral Management Services
MWD	=	measurement while drilling
P	=	pressure / hydrostatic pressure, psia

P_f = fracture pressure, psia

P_l = plastic limit

P_p = pore pressure, psia

PWD = pressure while drilling

S = overburden pressure, psia

SPE = Society of Petroleum Engineers

V_p = velocity of P-wave

V_s = velocity of S-wave

Greek Symbols

ε = normal strain, dimensionless

ε_a = axial strain, dimensionless

ε_H = horizontal strain, dimensionless

ε_{tr} = transverses strain, dimensionless

δ = displacement, ft

ρ = fluid density, lbm/gal

ρ_{air} = air density, lbm/gal

ρ_b = formation bulk density, lbm/gal

ρ_f = formation fluid density, lbm/gal

ρ_m = rock matrix density, lbm/gal

ρ_{sw} = seawater density, lbm/gal

ϕ = rock porosity, dimensionless

ϕ_D = density porosity, dimensionless

ϕ_s = sonic porosity, dimensionless

ν = Poisson's ratio

σ = effective stress, psi

σ_h = horizontal stress, psi

σ_v = vertical stress, psi

σ_{ob} = overburden stress, psi

σ_z = vertical effective stress, psi

REFERENCES

1. Danenberger, E.P.: “Outer Continental Shelf Drilling Blowouts,” paper OTC 7248 presented at the 1993 Offshore Technology Conference, Houston, 3-6 May.
2. Wojtanowicz, A.K., Bourgoyne, A.T., Zhou, D., and Bender, K.: “Strength and Fracture Gradients for Shallow Marine Sediments,” final report, U.S. MMS, Herndon (December, 2000).
3. Minerals Management Service (MMS): “Losses of Well Control,” www.mms.gov/incidents/blowouts.html, October 2004.
4. Reed, D.: “Shallow Geohazard Risk Mitigation; A Drilling Contractor’s Perspective,” paper IADC/SPE 74481 presented at the 2002 IADC/SPE Drilling Conference, Dallas, Texas, 26-28 February.
5. Adams, A.J. and Glover, S.B.: “An Investigation into the Application of QRA in Casing Design,” paper SPE 48319 presented at the 1998 SPE Applied Technology Workshop on Risk Based Design of Well Casing and Tubing, The Woodlands, Texas, 7-8 May.
6. Schuberth, P.C. and Walker, M.W.: “Shallow Water Flow Planning and Operations: Titan No. 1 Exploration Well, Deepwater Gulf of Mexico,” paper SPE 65751 presented at 1999 SPE/IADC Drilling Conference, Amsterdam, Holland, 9-11 March.
7. Goins, W.C. and Ables, G.L.: “The Causes of Shallow Gas Kicks,” paper SPE/IADC 16128 presented at the 1987 SPE/IADC Drilling Conference, New Orleans, Louisiana, 15-16 March.
8. Spencer, E.W.: *Introduction to the Structure of the Earth*, 2nd Edition, McGraw-Hill Book Company, New York (1977)**.**
9. Hornung, M.R.: “Kick Prevention, Detection, and Control: Planning and Training Guidelines for Drilling Deep High-Pressure Gas Well,” paper IADC/SPE 19990 presented at the 1990 IADC/SPE Drilling Conference, Houston, Texas, 27 February – 2 March.

10. Rollers, P.R.: “Riserless Drilling Performance in a Shallow Hazard Environment,” paper SPE/IADC 79878 presented at the 2003SPE/IADC Drilling Conferences, Amsterdam, The Netherlands, 19-21 February.
11. Huffman, A.R.: “The Future of Pressure Prediction Using Geophysical Methods,” AAPG Memoir **76**, 217-233.
12. Mukerji,T., Dutta, N., Prasad,M., and Dvorkin,J.:"Seismic Detection and Estimation of Overpressure, Part 1: the Rock Physics Basis," GSEG Recorder, (September 2002) 34-57.
13. Watson, D., Brittenham, T., and Moore, P.L.: Advanced Well Control, SPE Textbook Series, SPE, Richardson, Texas (2003), **10.**
14. Gramberg, J.: A Non-conventional View on Rock Mechanics and Fracture Mechanics, A.A.Balkema Publishers, Brookfield, Vermont (1989).
15. Bender, C.V., Bourgoyne, A.T., and Suhayda, J.N.: “Use of Soil Boring Data for Estimating Break-down Pressure of Shallow Marine Sediments,” paper presented at the 1994 IADC Well Control Conference of the Americas, Houston, Texas, 16-17 November.
16. Liang, Q.J.: “Application of Quantitative Risk Analysis to Pore Pressure and Fracture Gradient Prediction,” paper SPE 77354 presented at the 2002 SPE Annual Technical Conference and Exhibition, San Antonio, Texas, 29 September – 2 October.
17. Wojtanowicz, A.K. and Zhou, D.: “Shallow Casing Shoe Integrity Interpretation Technique,” paper SPE/IADC 67777 presented at the 2001 SPE/IADC Drilling Conference, Amsterdam, The Netherlands, 27 February – 1 March.
18. Eaton, B.A. and Eaton, T.L.: “Fracture Gradient Prediction for the New Generation,” World Oil, (October 1997) 93-100.
19. Barker, J.W. and Wood, T.D.: “Estimating Shallow Below Mudline Deepwater Gulf of Mexico Fracture Gradients,” paper presented at the 1997 Houston AADE Chapter Annual Technical Forum, Houston, Texas, 2-3 April.

20. Barker, J.W. and Meeks,W.R.: "Estimating Fracture Gradient in Gulf of Mexico Deepwater, Shallow, Massive Salt Sections," paper SPE 84552 presented at the 2003 SPE Annual Technical Conference and Exhibition, Denver, Colorado, 5-8 October.
21. Eaton, B.A.: “Using Pre-drill Seismic and LWD Data for Safe, Efficient Drilling,” www.worldoil.com/magazine/magazine_detail.asp?ART_ID=544, December 1998.
22. Hubbert, M.K. and Willis, D.G.: "Mechanics of Hydraulic Fracturing," *Trans.* AIME (1957) **210,** 153-168.
23. Mathews, W.R. and Kelly, J.: "How to Predict Formation Pressure and Fracture Gradient," *Oil and Gas J*, (1967) **65**, 8, 92-106.
24. Eaton, B.A.: "Fracture Gradient Prediction and its Application in Oil Field Operations," *JPT*, (1969) **21**, 1353-1360.
25. Eaton, B.A.: "Graphical Method Predicts Geopressures Worldwide," *World Oil*, **182**, (6), 51-56.
26. Anderson, R.A., Ingram, D.S., and Zanier, A.M.: "Determining Fracture Pressure Gradients from Well Logs," *JPT*, (1973) **25**, 11, 1259-1268.
27. Pilkington, P.E.: "Fracture Gradient Estimates in Tertiary Basins," *Petroleum Engineer International*, (1978) **50**, 5, 138-148.
28. Cesaroni, R., Giacca, D., Schenato, A., and Thierree, B.: "Determining Fracture Gradient While Drilling," *Petroleum Engineer International*, (1981) **53**, 7, 60-86.
29. Breckels, I.M. and Van Eeklelem, H.A.M.: "Relationship Between Horizontal Stress and Depth in Sedimentary Basins," paper SPE 10336 presented at the 1981 SPE Annual Technical Conference and Exhibition, San Antonio, Texas, 5-7 October.
30. Daines, S.R.: "Prediction of Fracture Pressure for Wildcat Wells," *JPT*, (1982) **34**, 4, 863-872.
31. Wiig, E. and Nesse, E.: "Environmental Quantitative Risk Assessment," paper SPE 35945 presented at the 1996 International Conference on Health, Safety and Environment, New Orleans, Louisiana, 9-12 June.

32. Vinnem, J.E.: “Environmental Risk Analysis of Near-hole Wildcat Well; Approach to Rational Risk Acceptance Criteria,” paper SPE 37852 presented at the 1997 SPE/UKOOA European Environmental Conference, Aberdeen, 15-18 April.
33. Newendrop, P.D. and Root, P.L.: “Risk Analysis in Drilling Investment Decisions,” paper SPE 1932 presented at the 1967 SPE Annual Fall Meeting, Houston, Texas, 1-4 October.

APPENDIX A

The step by step procedures to calculate Overburden Stress, Pore Pressure, and Horizontal Stress is:

1. To convert the measured soil boring density from grams per cubic centimeters to pounds mass per gallon:

$$\rho\left(\frac{g}{cc}\right)*8.3454043=\rho\left(\frac{lb_m}{gal}\right), \quad \text{.....(A.1)}$$

2. To calculate the air gap and sea water pressure gradient (g_{sw+sir}):

$$g_{sw+air}=\frac{0.052*D_{sw}*\rho_{sw}+0.052*D_a*\rho_{air}}{D_{sw}+D_a}, \quad \text{.....(A.2)}$$

3. To calculate the Overburden Stress gradient (g_{ob}) for SMS:

$$g_{ob}\left(\frac{psi}{ft}\right)=\frac{\rho_b\left(\frac{lbm}{gal}\right)}{19.25}, \quad \text{.....(A.3)}$$

4. To calculate the Overburden Stress gradient (g_{ob}) for deeper sediments; (Caution: this equation is an approximation)

$$g_{ob}=0.84753+0.01494\frac{D_{se}}{1000}-0.0006\left(\frac{D_{se}}{1000}\right)^2+1.199\times10^{-5}\left(\frac{D_{se}}{1000}\right)^3, \quad \text{.....(A.4)}$$

5. To calculate the Equivalent Sediment depth by using Eq. 21 and Eq. 22.

$$D_{s(eq)}\approx\frac{D_{sw}}{2}, \quad \text{.....(A.5)}$$

$$D_{se}=D_{s(eq)}+D_s, \quad \text{.....(A.6)}$$

6. To calculate Poisson's ration based on Seismic data or assume Poisson's ratio for the location (only if the seismic data is not applicable)

$$\nu = 0.5\frac{\left(\frac{V_P^2}{V_S^2} - 2\right)}{\left(\frac{V_P^2}{V_S^2} - 1\right)}, \quad \text{.....(A.7)}$$

7. To calculate the Overburden Stress (δ_{ob}):

$$D_{below} * g_{ob} + \left(D_a + D_{sw}\right) * g_{sw+air} = \delta_{ob}, \quad \text{.....(A.8)}$$

8. To calculate the Pore Pressure (P_p):

$$D_{below} * g_{P_p} + \left(D_a + D_{sw}\right) * g_{sw+air} = P_p, \quad \text{.....(A.9)}$$

9. To calculate the Horizontal Stress (δ_H) by using Eq. 7.

$$\sigma_H = \left(\frac{\nu}{1-\nu}\right)\left(\sigma_{ob} - P_p\right) + P_p, \quad \text{.....(A.10)}$$

10. Plot calculated Horizontal Stress (δ_H), Pore-Pressure (P_p) and Overburden Stress(δ_{ob}) vs. Depth below mudline.

D_{sw}	300	ft	ν_1	0.1
g_{Pp}	0.465	psi/ft	ν_2	0.2
Air-Gap	70	ft	ν_3	0.3
g_{sw+air}	0.363	psi/ft	ν_4	0.4
			ν_5	0.5
			ν_6	0.6

D_{below}	ρ	ρ	g_{ob}	δ_{ob}	Pp	δ_{H3}
ft	gm/cc	lbm/gal	psi/ft	psi	psi	psi
9.2	1.5234	12.71	0.6604	140.27	138.48	139.25
14.45	1.5559	12.98	0.6745	143.94	140.92	142.21
20.37	1.6201	13.52	0.7024	148.50	143.67	145.74
24.97	1.6676	13.92	0.7230	152.25	145.81	148.57
31.54	1.7476	14.58	0.7576	158.09	148.86	152.82
34.17	1.6201	13.52	0.7024	158.20	150.09	153.56
36.79	1.9409	16.20	0.8414	165.15	151.30	157.24
37.45	1.9726	16.46	0.8552	166.22	151.61	157.87
45.99	1.7326	14.46	0.7511	168.74	155.58	161.22
49.93	1.7167	14.33	0.7442	171.36	157.41	163.39
59.79	1.7484	14.59	0.7580	179.52	162.00	169.51
70.3	1.7001	14.19	0.7370	186.01	166.89	175.08
80.16	1.6526	13.79	0.7164	191.63	171.47	180.11
90.01	1.7001	14.19	0.7370	200.54	176.05	186.55
110.38	1.7167	14.33	0.7442	216.35	185.52	198.73
120.24	1.6676	13.92	0.7230	221.12	190.11	203.40
133.38	1.9726	16.46	0.8552	248.26	196.22	218.52
139.29	2.0526	17.13	0.8899	258.15	198.97	224.33
249.67	1.9726	16.46	0.8552	347.71	250.29	292.04
329.83	1.8609	15.53	0.8068	400.29	287.57	335.88
341.66	1.9409	16.20	0.8414	421.68	293.07	348.19
350.2	1.9409	16.20	0.8414	428.87	297.04	353.54
359.55	1.9077	15.92	0.8270	431.56	301.39	357.18
360.05	1.9085	15.93	0.8274	432.10	301.62	357.54

Figure A- 1 Data and Results for the Grand Isle 4, GOM

D_{sw}	300	ft	ν_1	0.1
g_{Pp}	0.465	psi/ft	ν_2	0.2
Air-Gap	70	ft	ν_3	0.3
g_{sw+air}	0.363	psi/ft	ν_4	0.4
			ν_5	0.5
			ν_6	0.6

D_{below}	ρ	ρ	g_{ob}	δ_{ob}	Pp	δ_{H3}
ft	gm/cc	lbm/gal	psi/ft	psi	psi	psi
10.51	1.5559	12.9846	0.6745	141.29	139.08	140.03
22.34	1.6367	13.6589	0.7096	150.05	144.59	146.93
32.19	1.6359	13.6522	0.7092	157.03	149.17	152.53
40.74	1.6526	13.7916	0.7164	163.39	153.14	157.53
55.19	1.7159	14.3199	0.7439	175.25	159.86	166.46
65.05	1.6676	13.9168	0.7230	181.23	164.45	171.64
75.56	1.7001	14.1880	0.7370	189.89	169.33	178.14
86.07	1.6835	14.0495	0.7298	197.01	174.22	183.99
96.58	1.6835	14.0495	0.7298	204.69	179.11	190.07
126.15	2.1002	17.5270	0.9105	249.06	192.86	216.94
136.01	2.0043	16.7267	0.8689	252.38	197.44	220.99
166.23	1.9401	16.1909	0.8411	274.01	211.49	238.29
196.45	2.0851	17.4010	0.9039	311.78	225.55	262.50
206.96	2.0851	17.4010	0.9039	321.28	230.43	269.37
226.68	1.9893	16.6015	0.8624	329.69	239.60	278.21
268.73	2.0360	16.9912	0.8827	371.39	259.16	307.26

Figure A- 2 Data and Results for the Grand Isle Block 43, GOM

D_{sw}	300	ft	ν_1	0.1
g_{Pp}	0.465	psi/ft	ν_2	0.2
Air-Gap	70	ft	ν_3	0.3
g_{sw+air}	0.363	psi/ft	ν_4	0.4
			ν_5	0.5
			ν_6	0.6

D_{below}	ρ	ρ	g_{ob}	δ_{ob}	Pp	δ_{H3}
ft	gm/cc	lbm/gal	psi/ft	psi	psi	psi
9.86	1.4917	12.44884	0.646693	140.57	138.78	139.55
14.45	1.5242	12.72007	0.660783	143.75	140.92	142.13
19.71	1.5717	13.11647	0.681375	147.63	143.36	145.19
24.97	1.5876	13.24916	0.688268	151.38	145.81	148.20
29.57	1.6209	13.52707	0.702705	154.98	147.95	150.96
38.76	1.5876	13.24916	0.688268	160.87	152.22	155.93
48.62	1.6201	13.52039	0.702358	168.35	156.81	161.75
59.13	1.6676	13.9168	0.72295	176.95	161.69	168.23
70.3	1.6842	14.05533	0.730147	185.53	166.89	174.88
80.16	1.6526	13.79162	0.716448	191.63	171.47	180.11
90.01	2.021	16.86606	0.876159	213.06	176.05	191.91
93.96	2.0051	16.73337	0.869266	215.87	177.89	194.17
100.53	2.0368	16.99792	0.883009	222.97	180.94	198.95
105.12	2.101	17.53369	0.910841	229.94	183.08	203.16

Figure A- 3 Data and Results for the West Delta Block 70, GOM

D_{sw}	300	ft	ν_1	0.1
g_{Pp}	0.465	psi/ft	ν_2	0.2
Air-Gap	70	ft	ν_3	0.3
g_{sw+air}	0.363	psi/ft	ν_4	0.4
			ν_5	0.5
			ν_6	0.6

D_{below}	ρ	ρ	g_{ob}	δ_{ob}	Pp	δ_{H3}
ft	gm/cc	lbm/gal	psi/ft	psi	psi	psi
1.31	1.5876	13.2492	0.6883	135.10	134.81	134.93
3.94	1.5884	13.2558	0.6886	136.91	136.03	136.41
7.23	1.6042	13.3877	0.6955	139.23	137.56	138.27
9.86	1.6359	13.6522	0.7092	141.19	138.78	139.81
13.14	1.6042	13.3877	0.6955	143.34	140.31	141.61
15.77	1.6042	13.3877	0.6955	145.16	141.53	143.09
31.54	1.5559	12.9846	0.6745	155.47	148.86	151.70
47.96	1.5717	13.1165	0.6814	166.88	156.50	160.95
53.22	1.6359	13.6522	0.7092	171.94	158.94	164.51
63.07	1.7001	14.1880	0.7370	180.68	163.52	170.88
68.33	1.6042	13.3877	0.6955	181.72	165.97	172.72
78.19	1.6842	14.0553	0.7301	191.29	170.56	179.44
88.7	1.6526	13.7916	0.7164	197.75	175.44	185.00
93.96	1.7001	14.1880	0.7370	203.45	177.89	188.84
108.41	1.6034	13.3810	0.6951	209.55	184.61	195.30
137.32	1.8768	15.6627	0.8136	245.93	198.05	218.57
178.06	1.7167	14.3266	0.7442	266.72	217.00	238.30
188.57	1.7643	14.7238	0.7649	278.43	221.88	246.12
208.28	1.7643	14.7238	0.7649	293.50	231.05	257.81
218.13	1.7009	14.1947	0.7374	295.04	235.63	261.09
228.65	1.7476	14.5844	0.7576	307.43	240.52	269.20
258.21	1.9251	16.0657	0.8346	349.70	254.26	295.16
268.73	1.8926	15.7945	0.8205	354.69	259.16	300.10
277.92	1.9085	15.9272	0.8274	364.14	263.43	306.59
288.44	1.7326	14.4592	0.7511	350.85	268.32	303.69
318	1.8459	15.4048	0.8002	388.68	282.07	327.76
318.66	1.9893	16.6015	0.8624	409.01	282.37	336.65
328.52	1.9085	15.9272	0.8274	406.01	286.96	337.98
337.71	1.9409	16.1976	0.8414	418.36	291.23	345.71
348.23	1.9726	16.4621	0.8552	432.00	296.12	354.35
358.74	1.9568	16.3303	0.8483	438.53	301.01	359.95
367.94	1.9885	16.5948	0.8621	451.39	305.29	367.90
377.79	1.6842	14.0553	0.7301	410.04	309.87	352.80
388.3	1.8768	15.6627	0.8136	450.14	314.76	372.78
398.16	1.8776	15.6693	0.8140	458.30	319.34	378.89

Figure A- 4 Data and Results for the Ship Shoal Block 198, GOM

D_{sw}	300	ft	ν_1	0.1
g_{Pp}	0.465	psi/ft	ν_2	0.2
Air-Gap	70	ft	ν_3	0.3
g_{sw+air}	0.363	psi/ft	ν_4	0.4
			ν_5	0.5
			ν_6	0.6

D_{below}	ρ	ρ	g_{ob}	δ_{ob}	Pp	δ_{H3}
ft	gm/cc	lbm/gal	psi/ft	psi	psi	psi
10.51	1.5076	12.5815	0.6536	141.07	139.08	139.93
20.37	1.5393	12.8461	0.6673	147.79	143.67	145.44
21.02	1.4434	12.0458	0.6258	147.35	143.97	145.42
28.91	1.5725	13.1231	0.6817	153.91	147.64	150.33
36.14	1.5725	13.1231	0.6817	158.83	151.00	154.36
38.76	1.5725	13.1231	0.6817	160.62	152.22	155.82
48.62	1.6042	13.3877	0.6955	168.01	156.81	161.61
57.82	1.5551	12.9779	0.6742	173.18	161.08	166.27
69.65	1.5393	12.8461	0.6673	180.68	166.58	172.62
78.84	1.5567	12.9913	0.6749	187.40	170.86	177.95
91.33	1.6209	13.5271	0.7027	198.38	176.67	185.97
99.87	1.6526	13.7916	0.7164	205.75	180.64	191.40
105.78	1.6526	13.7916	0.7164	209.98	183.38	194.78
111.7	1.6526	13.7916	0.7164	214.22	186.14	198.17
120.89	1.6359	13.6522	0.7092	219.93	190.41	203.06
139.95	1.6217	13.5337	0.7031	232.59	199.27	213.55
151.12	1.7318	14.4526	0.7508	247.66	204.47	222.98
159.66	1.7967	14.9942	0.7789	258.56	208.44	229.92
190.54	1.7809	14.8623	0.7721	281.31	222.80	247.87
208.94	1.6692	13.9301	0.7236	285.40	231.35	254.51
241.13	1.7960	14.9883	0.7786	321.94	246.32	278.73
250.33	1.7801	14.8557	0.7717	327.38	250.60	283.51
270.7	1.7484	14.5911	0.7580	339.38	260.07	294.06
319.32	1.8926	15.7945	0.8205	396.20	282.68	331.33
330.49	1.8451	15.3981	0.7999	398.56	287.88	335.31
339.03	1.8776	15.6693	0.8140	410.16	291.85	342.55
350.85	1.9560	16.3236	0.8480	431.71	297.34	354.93
360.05	1.7967	14.9942	0.7789	414.65	301.62	350.06
389.62	1.7167	14.3266	0.7442	424.17	315.37	362.00
389.62	1.7167	14.3266	0.7442	424.17	315.37	362.00
400.13	1.7492	14.5978	0.7583	437.63	320.26	370.56
409.99	1.7318	14.4526	0.7508	442.01	324.84	375.06
417.21	1.7349	14.4784	0.7521	447.99	328.20	379.54
421.16	1.7326	14.4592	0.7511	450.54	330.04	381.68
444.81	1.8760	15.6560	0.8133	495.96	341.03	407.43

Figure A- 5 Data and Results for the Ship Shoal Block 307, GOM

VITA

Name:	Yong B. Tu
Born:	October 6, 1975, Shanghai, People's Republic of China
Address:	3305 Ross Cove Round Rock Texas, USA
Education:	Texas A&M University Bachelor of Science – Ocean Engineering (1998) Texas A&M University Mater of Science – Petroleum Engineering (2005)